

Rotating Tool Cold Expansion

Motali Bhoopati Kumar

A Dissertation Submitted to
Indian Institute of Technology Hyderabad
In Partial Fulfillment of the Requirements for
The Degree of Master of Technology



भारतीय प्रौद्योगिकी संस्थान हैदराबाद
Indian Institute of Technology Hyderabad

Department of Mechanical Engineering

May, 2013

Declaration

I declare that this written submission represents my ideas in my own words, and where others' ideas or words have been included, I have adequately cited and referenced the original sources. I also declare that I have adhered to all principles of academic honesty and integrity and have not misrepresented or fabricated or falsified any idea/data/fact/source in my submission. I understand that any violation of the above will be a cause for disciplinary action by the Institute and can also evoke penal action from the sources that have thus not been properly cited, or from whom proper permission has not been taken when needed.



(Signature)

MOTALI BHOPATI KUMAR

(- Student Name -)

ME10M03

(Roll No)

Approval Sheet

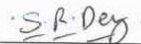
This thesis entitled “Rotating tool cold expansion” by **Motali Bhoopati Kumar** is approved for the degree of Master of Technology from IIT Hyderabad.



-Name and affiliation-
Examiner



-Name and affiliation-
Examiner



-Name and affiliation-
Chairman

(Dr. Suhas Ranjan DEY)
Assistant Professor
Department of Materials Science
and Engineering

Acknowledgements

With immense pleasure I express my deep and sincere gratitude, regards and thanks to my thesis advisor **Dr. Abhay Sharma** for his excellent guidance, invaluable suggestions and continuous encouragement at all the stages of my research work. His wide knowledge and logical way of thinking have been of great value for me. As a guide he has a great influence on me, both as a person and as a professional. I am able to complete my project successfully with his support.

I would like to thank **Prof Desai** Director of IIT Hyderabad and **Prof Vinayaka Eswaran** HOD for Department of Mechanical Engineering for approving this project and guiding, encouraging me all through the course of the project.

It was a great pleasure to me as a part of Department of Mechanical, IIT Hyderabad and I would like to thank all the staff members and my friends for helping me in all stages of my work and making the great place to work in.

I would also like to thank my batch mates **Vinay, Sathish, Rahul, Vikranth, Pruthvi, Bagath Singh, Nitin panskar** and all **M Tech** friends for their moral support and sharing of knowledge which has been helpful to me so far. Special thanks goes to Ph.D scholars **Somashekara, Nilanjan** and **Sri lakshmi** for providing me support at the hard times of my research work. I would like to thank **Moulali, Dananjay sahuo** and **Madhu** for helping me in the Work shop and CAE lab. Being with the friends in IIT Hyderabad was a nice experience which will be most memorable part of my entire life. The days I have spent in IIT H has been very nurturing and educating me.

I specially thank Mr. **Guru Prasath Ravindran** (Project Associate 2011-12), who supported me morally a lot at the time of my illness and taken care as a brother.

Above all, I extend my deepest gratitude to **my parents** and **my grandfather Late M. Jangaiah** for their invaluable love, affection, encouragement and support.

Dedicated to

My Parents

&

My Grand Father

Abstract

Many engineering parts in industries are assembled by rivets, bolts, pins etc. These joints are more vulnerable to fatigue loadings and a crack is emanated. As structure is in use crack starts propagating over a period of time. Crack propagation can be obstructed by inducing a compressive residual stress zone around the vulnerable parts. Cold expansion hole (CEH) is one of the techniques used to induce compressive stress zone, by inserting a tapered pin or a large diameter ball into an undersized hole. As the oversized object is inserted into the hole, the surrounding material is elastically deformed and when the object comes out from the other side, the expanded material springs back to form tangential compressive residual stress around the hole. In most of the cases the crack originates on the surface, a good surface finish is also an important parameter for increasing the strength at the surface and stop crack emanation. However, good surface finish is not achieved by CEH. A novel technique called rotating tool cold expansion (RTCE) technique is developed where a tapered mandrel is inserted into an undersized hole besides rotating it simultaneously. The tool rotation breaks down the coarse grains into fine grain structure achieving good surface finish. In this method, RTCE is performed with three undersized diameters, namely, 9.2, 9.5 and 9.9 mm diameters to a maximum of 10 mm diameter. The tool material is high speed steel and the work piece material is commercial aluminium. The induced residual stresses are measured using X-ray diffraction method and compared for three different Cold expansion holes. Due to the rotation of the tool, heat is generated because of both friction at the interface and plastic deformation. A 3-D thermo-mechanical analysis is performed in ANSYS FEA for different values of coefficient of friction and plastic deformation rate and validated with experimental results. Compared to the degree of cold expansion through conventional techniques (upto 4%) the proposed technique is capable to produce good results up to 8.69% of cold expansion. Role of heat generated through friction and plastic deformation is critical to attain the best possible result, equal contributions of both are important.

Nomenclature

Symbol	Description	Unit
μ	Coefficient of friction	--
δ	Slip rate	--
\dot{Q}	Heat generation rate	Nm/s
\dot{q}	Heat Flux Rate	N/ms
r	Radius	M
ω	Angular velocity	rad/s
σ_y	Yield stress	N/m ²
τ	Contact shear stress	N/m ²

Contents

Declaration.....	Error! Bookmark not defined.
Approval Sheet	Error! Bookmark not defined.
Acknowledgements	iv
Abstract.....	vi
Nomenclature	vii
1 Introduction	1
2 Background	5
2.1 Literature review.....	5
2.2 Previous studies on modelling.....	9
2.3 Gaps and opportunities	10
3 Experimental	11
3.1 Rotating tool cold expansion hole	11
3.2 Experimental setup	13
4 Numerical modelling	16
4.1 Heat generation model.....	16
4.2 Tool motion	19
4.3 Contact Pressure model	20
4.4 Simulation.....	21
5 Results and Discussion	25
5.1 Variation of residual Stress through thickness	25
5.2 At the role of μ and δ	27
6 Conclusion	32
6.1 Scope of future.....	32
References	33
Appendix	36

List of Figures		Pg. No.
1	Various cold expansion methods	2
2	Surface mechanical attrition treatment	8
3(a)	RTCE process	12
3(b)	Three different tools of diameter 9.2, 9.5 and 9.9mm	12
4	Experimental Setup	13
5	Force variation F_y with time, initial diameter 9.9mm	14
6	The residual stress variation for tool diameter 9.9mm	14
7	Tool position at different times during RTCE process	19
8	Pressure variation with time for tool initial diameter 9.5mm	21
9	A half section symmetrical 3 D model	22
10	Stress-Strain curve of pure aluminum at different temperatures	22
11	Tangential residual stress profile for 9.5 tool $\mu=0.1$ $\delta=0.5$	23
12	Simulation results at different sections, tool initial diameter 9.5 mm	26
13	Experimental results at top and bottom plane of the work piece	27
14	Residual stress variation with different tools	28
15	Experimental setup showing three different conditions	29
16	Maximum compressive residual stresses under three different conditions for all DCE	30

List of Tables

List of Tables		
1	Maximum residual stress induced in the RTCE process near the hole for three different DCE	15
2	Area of contact at different instants of time	20
3	Error in predicted residual stress at different δ and μ with tool diameter 9.5 mm	24
4	Results showing the maximum compressive residual stress when compared to experimental value	31
5	Error in predicted residual stress at different δ and μ	31

Chapter 1

Introduction

In aircraft and many other structural components bolts, rivets and pins are widely used for connecting different assemblies. The presence of holes in the in-service components may lead to high stress concentration around these holes. When the material under high stress concentration is subjected to cyclic loading, initiation and growth of cracks accelerates resulting in early failure of the component. Therefore it is important to strengthen the material at these high stress concentration zones. In general, tensile stresses propagate the crack and compressive stress retards the crack growth. Thus, the life of a component under static or dynamic load can be improved by enhancing the compressive stresses around the crack emanating zones. Cold expansion hole (CEH) is one of the processes which have been commonly used to improve the fatigue life of fastener holes for past 40 years. Cold expansion is a mechanical process in which an undersized hole is compressed radially outwards by insertion of an oversized tool. The CEH provides a beneficial compressive residual stresses around fastener holes in a way that delay fatigue crack initiation and growth, leading to an extension in the fatigue life of components.

There are many ways to perform cold expansion among which the well-known include tapered pin, oversized ball, split sleeve and spherical mandrel. The following are few well known. In traditional cold expansion an oversized tapered pin is forced through a hole, as shown in figure 1(a), applies lateral pressure on the surface which locally yields the material to create a plastic region around the hole. When the tool comes out of the hole, the elastically deformed surrounding material springs back from the expanded state and the resulting contraction leads to compressive tangential residual stress around the hole [1].

Another cold expansion process, known as ballising, involves inserting a ball, through an undersized pre-machined hole as shown in figure 1(b). Ballising is a line contact unlike the tapered tool in which the entire inner surface remains in contact. During ballising process the surface of the hole is compressed and work hardened. There is a limitation that the contact of the ball or tapered mandrel may damage the surface finish. Hence the cold expansion operation is generally followed by a reaming operation.

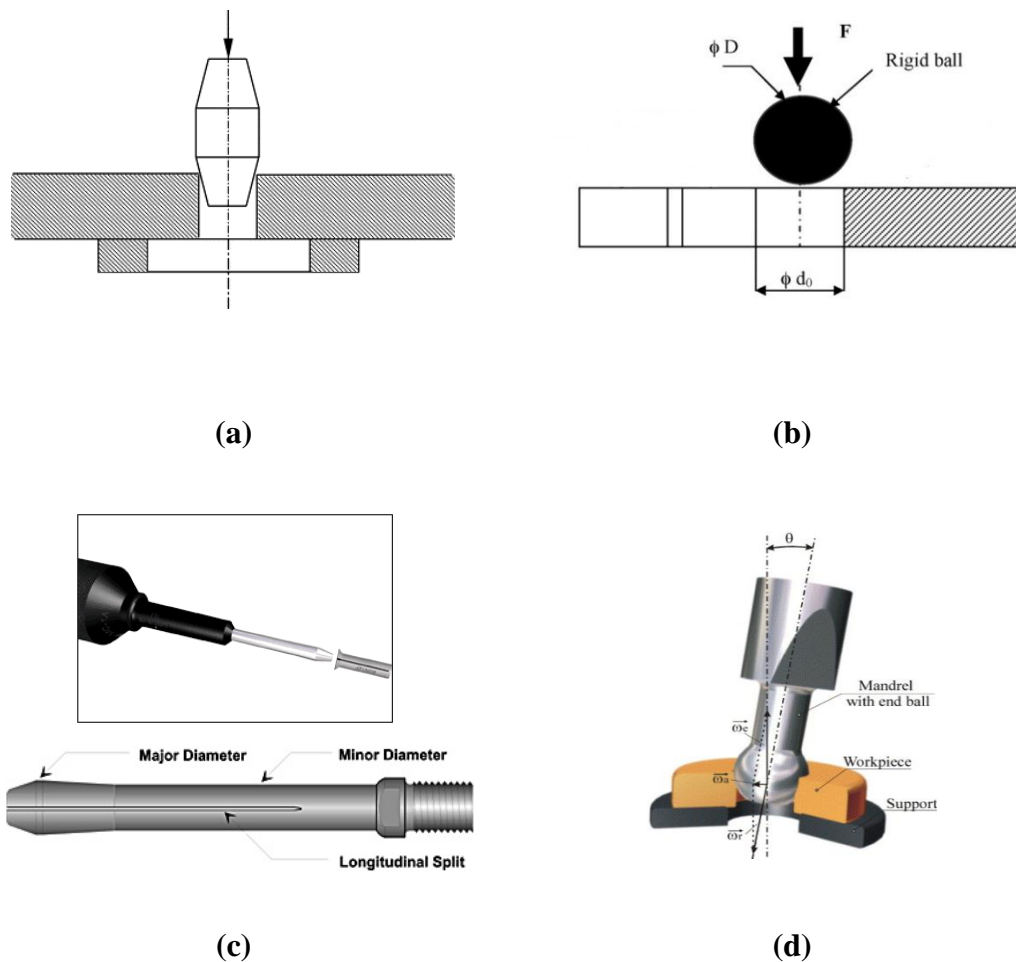


Figure 1: Various cold expansion methods {(a) Tapered tool [1], (b) ballising [19], (c) Split Sleeve method [http://www.fatiguetech.com/coldEX_Split_sleeve.html], (d) Spherical Method [3]}

In order to prevent the surface damage other variants of cold expansion like split sleeve and split mandrels are used [2], as shown in figure 1(c) and 1(d). In the split

sleeve, a sleeve is placed over the tapered mandrel and both together inserted into the hole. The hole is expanded when the large diameter of the mandrel is drawn back through the sleeve. The sleeve is then removed from the hole and discarded. The sleeveless split mandrel process consists of a hollow longitudinally slotted tapered mandrel. The sleeveless split, is inserted into the hole and a pilot is pushed through the hollow portion, expanding the hole. Solid lubricants are used with the split sleeve and the split mandrel methods are used to prevent the surface damage. Another lubricant method of cold expansion is spherical mandrel [3], in which good surface finish is achieved in previously drilled round holes by means of surface plastic or volumetric plastic deformation. The tool performs rectilinear translation along the hole axis, rotates round its own axis and simultaneously it rotates round the axis of the hole being formed.

The effectiveness of cold expanded holes significantly depends on the amount of induced compressive residual stress around the hole and the surface finish of the internal wall as well. Generally fatigue cracks initiates at the free surfaces due to geometric discontinuity and surface roughness.

As most of the fatigue failures occur on the free surface, it is well recognized that the fatigue life of a component is very much dependent on the surface finish. The fatigue life can also be improved by recently developed techniques like friction stir processing (FSP) in which a defect free recrystallized fine micro-structure is formed at the surface through severe plastic deformation [4]. In the FSP a specially designed cylindrical tool is rotated and plunged into the selected area. The tool has a small diameter pin with a concentric larger diameter shoulder. The rotating pin contacts the surface and vigorously stir it without changing the phase and breaks down the coarse microstructure to fine. Moreover, additive particles can also be dispersed on the surface which embeds to the base material due to the FSP and improves the tensile strength, ductility and fatigue life of component made of alloys [5] and cast materials [6]. Such improvement in the surface properties are also essential for the holes produced by the foregoing cold expansion hole techniques.

Thus considering the advantage of both cold expansion process and friction stir processing a new process is developed called rotating tool cold expansion (RTCE). A tapered tool is rotated and simultaneously inserted in to the undersized hole.

Insertion of a tapered tool causes cold expansion process and the rotation of tool causes stirring action on the surface which breaks down the coarse grain into fine microstructure. The subsequent chapters give details on the RTCE in to the RTCE as follows.

- ‘Background’ describes the existence of cold expansion and surface finishing processes like friction stir processing.
- ‘Experimental’ describes the complete procedure followed for RTCE process.
- ‘Numerical Modelling’ explains the model developed for the RTCE based on the physics behind the process and also explains the simulation procedure.
- ‘Results and discussion’ discusses about the role of parameters of plastic deformation and coefficient of friction and variation of residual stress through thickness. Also discusses the results obtained under different conditions of the experiment.
- Finally this report is concluded in chapter titled ‘Conclusions’ with the recommendations for future work.

Chapter 2

Background

Cold expansion hole (CEH) processes have been commonly used to improve the fatigue life of fastener holes since past 40 years. This process was developed by Boeing Company and is presently being marketed by Fatigue Technology Inc. (FTI). A vast development has been taken place in this technology, to increase the fatigue strength in all required zones of the components and has a huge application in aerospace. Later, recent times focus has been made in modifying the surface texture which inherently produces the fatigue strength. The surface-engineering technology developed a new process called Friction-stir processing (FSP) which refine microstructures, thereby improving strength and ductility, increase resistance to corrosion and fatigue. Friction stir processing emerged from Friction stir welding, developed by the welding Institute UK in 1991. In Friction stir welding the two metals are joined by softening of the material at interface, due to rotating tool, and applying pressure. The weld mixes the material without changing the phase and a fine micro-structure is observed in the weld zone. In the present chapter the background of the problem is described through reviewing the literature and the problem statement is defined through finding the gaps and opportunities.

2.1 Literature review

Kliman et al. [7] developed a procedure to determine the optimal pre-strain value based on the material stress-strain and stress concentration factor. The residual stress, stress-strain curve transformation and microstructural influence are quantified, and the optimal residual strain yielding the maximum fatigue limit improvement is computed. They developed a model of fatigue life enhancement

by means of cold hole expansion and experimentally verified exploiting the mandrelizing technological process with a rotating and non-rotating mandrel.

Liu et al. [8] conducted direct cold expansion hole on aluminium alloy 2A12T4 open holes. The fatigue tests reveal that direct cold expansion technique could elevate about six times fatigue life. But the tangential residual stress distribution around hole is non-axisymmetric.

In general, it is found that in conventional direct cold expansion method a non-uniform residual stress distribution is formed through the plate thickness and even tensile residual stress can be created at the entrance and exit faces once the ball is removed. Chakherlou et al. [9] proposed a new novel method of cold expansion where a tapered pin is inserted with a mating tapered split sleeve which creates an almost uniform compressive residual stress around the hole. A 3D FEA method has been used to calculate tangential residual stress around a cold-expanded hole using a tapered pin with a mating tapered split sleeve.

The fatigue life of a component can be predicted based on the residual stress profile. X-ray diffraction and 3D finite element analysis (FEA) can be used to determine the residual stress profile. P.F.P. de Matos [10] studied the residual stress effect due to cold-working in relation to fatigue striation spacing. Scanning electron microscopy (SEM) measurements were performed for measuring the striation spacing. Fatigue striation spacing measurements along the crack length for two open hole specimens with and without residual stress were presented and the results shown that fatigue striation spacing along the crack length decrease due to the residual stress effect.

Repair of aircraft structures is a key component to extend aircraft service life. Re-cold expansion process conditions such as the degree of cold expansion should be determined to impart the beneficial compressive residual stresses around the holes under tensile loadings. Jang [11] developed a process simulation using three-dimensional finite element analysis to determine the residual stress imparted by re-cold expansion in the fastener holes under the external loading conditions. Three levels of re-cold expansion under three external loading levels are determined and shown that the re-cold expansion process with at least 6 percent of the degree of cold expansion imparts deep residual stresses around the hole so that the resulting

stress levels on the hole entry side remain compressive under applied external stress levels between 100 and 200MPa.

Fatigue life of a component is also adversely affected by surface roughness. Surface properties can be improved by a novel friction stir process. Friction stir processing (FSP), developed by Mishra et al. [4] provides the ability to thermo-mechanically process selective locations on the structure's surface and enhance specific properties and modify the local microstructure without joining the metals together. A specially designed cylindrical tool is rotated and plunged into the selected area. The vigorous stirring action of the tool mixes the material without changing the phase (by melting or otherwise) and breaks down the coarse microstructure to fine-equiaxed grains.

Friction stir processing (FSP) of cast Mg–9Al–1Zn alloy plus subsequent aging produced a defect-free recrystallized fine-grained microstructure with fine β -Mg₁₇Al₁₂ particles. In D. Wang et al. [12] experiment on FSP, the processed sample exhibited significantly enhanced fatigue properties compared to the as-cast parent material, with the fatigue strength being increased from 45-95MPa and the fracture mode being changed from quasi-cleavage fracture to dimple fracture. The improvement was attributed to refinement of grains, elimination of porosities and coarse networks, and precipitation of fine particles.

Friction stir processing enhances the tensile strength and fatigue strength of the metal. Hossein et al. [5] performed friction stir processing by dispersing and embedding TiB₂ particles with global size of 2.62 μ m in Al7075 and the corresponding tensile test result shows rising in yield strength by more than two times of base metal.

Metallic parts produced by casting are often subjected to metallurgical flaws like porosity and microstructural defects. Friction stir processing can be used to introduce wrought microstructure/Nano-particles into a cast component and eliminate many of the defects. Grain refinement, homogenization of the microstructure and the elimination of porosity improves the fatigue life. Sharma [6] investigated fatigue test for Cast A356 alloys prepared by friction stir processing (FSP) and results showed a significant improvement in fatigue life of A356. FSP can be used as a tool to locally modify the microstructures in the regions of high fatigue

loading and thus significantly improve the overall performance of aluminum castings.

Severe plastic deformation (SPD) processes involves very large strains in the material in the presence of a high hydrostatic pressure without causing any changes in the dimensions of the work piece. The preservation of shape is achieved due to special tool geometries which prevent the free flow of material and thereby produce a significant hydrostatic pressure essential for producing high densities of crystal lattice defects, particularly dislocations, which can result in a significant refining of the grains. However, bulk deformation and high energy consumption is not desirable. An alternative convenient method of improving the surface texture is surface mechanical attrition treatment (SMAT). SMAT improves mechanical properties of metallic materials through the formation of Nano crystallites at their surface layer. SMAT process involves a specimen placed in a tubular chamber with a dimension of length 150 mm and diameter 80 mm along with 250 stainless steel milling balls [13] as shown in figure 2. In the SMAT process the chamber is vibrated for about 20 minutes such that a multiple impact between the specimen and milling balls takes place. The SMAT increase the subsurface micro hardness of the steel.

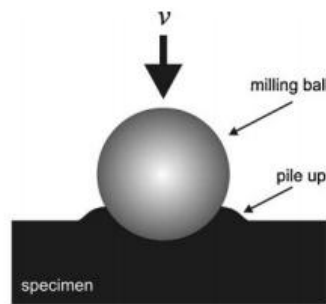


Figure 2: Surface mechanical attrition treatment

Spherical mandrelling (SM) is a new method of forming round good finished predrilled holes by surface plastic or volumetric plastic deformation. In the second case the hole undergoes cold expansion. The tool rotates around its own axis at and at the same time it rotates around axis of the hole being formed. Simultaneously, the tool translates on the axis of the hole. The SM specific kinematics allows the formation of a natural hydrodynamic wedge of the lubricant between the tool and

work piece. As a result, there are no bruises and seizures on the worked surface, which might enhance the susceptibility of the material to form fatigue cracks. Maximov et al. [14] developed an optimized 3D finite element (FE) model of the cold hole expansion process by means of spherical mandrelling (SM) and used for investigation of the residual displacements and stresses around cold expanded holes. The study developed an all-purpose 3D FE model of the SM process with a view of its application to work pieces with different shape, sizes and material characteristics. An advantage of SM is it can be carried out on both non-conventional and conventional (milling and drilling) machines and it considerably increases their technological potentials. Shamdani et al. [15] investigated numerical study using FEA software for the combined cold expansion and local torsion on fastener holes. The local torsion can be considered as a localized SPD process.

2.2 Previous studies on modelling

Numerical studies have been published for different variants of cold expansion techniques like tapered pin [1,8,17,18], ballising [19,20], split sleeve [21] and spherical mandrelling [14] etc. One of the recent investigations presented numerical studies on cold expansion followed by local torsion [15]. Most of the FEA models for the foregoing variants have been attempted through different approaches including 2D strain/stress, 2D axisymmetric, 3D uniform expansion etc. However, in reality the cold expansion takes place sequentially through the axial motion of the oversized mandrel rather than uniformly [21]. One of the different approaches developed by Babu et al. [22] considers staggered application of displacement independently at different layers. This approach provides a better approximation [21]. In the present work we have used similar approach however the process of RTCE is considerably different because of the simultaneous frictional stirring along with the cold expansion. Our understanding about the mechanics of such complex combination is limited. The proportion of frictional stirring and cold expansion, the effect of degree of cold expansion, the thickness effect are some of the questions the present work attempts to answer. The prime objective is to unearth the physics behind the RTCE process through numerical modelling supported by experimentation.

2.3 Gaps and opportunity

Recent technologies reviewed that in addition to cold expansion hole, a good surface finish may lead to a better fatigue life. More surface roughness is conducive to initiation of cracks, thus reducing the effect of fatigue strength. Altering the surface texture has not been attempted so far. Modelling of torque during cold expansion has been reported but a comprehensive model of rotating tool cold expansion with experimental validation is not available. Another drawback to overcome is the current cold expansion technique has got a heavy setup.

The moot point is whether the conventional CEH techniques may be amalgamated with the aforesaid severe plastic deformation. The present work is a fundamental attempt to assess the feasibility of such amalgamation. Unlike the rectilinear translation of the tapered tool during the conventional CEH the tapered tool in the present work also rotates while inserting. The rotation is envisaged to stir the surface and produce beneficial alteration in the surface properties causing stirring action on the inner surface of the hole. A numerical study supported by experimentation is carried out to understand the physics behind the rotating tool cold expansion (RTCE).

Chapter 3

Experimental

The experimental setup required for the RTCE is a simple CNC vertical milling machine. The experimental procedure involves the RTCE process, force measurement at the time of the process followed by residual stress measurement of the sample. The measured force is used as an input in the simulation work. The induced residual stresses decide the fatigue strength of the material. So, further experimental procedure extends up to fatigue testing, though it is not done in the current work.

3.1 Rotating Tool Cold Expansion Hole

The process of rotating tool cold expansion includes a tapered tool which is mounted on vertical machining center. The tool rotates and simultaneously inserts into the undersized hole as shown in figure 3 (a). Prior to the RTCE, the predrilled hole is also produced on the same vertical machining center. Thus, unlike the conventional tapered tool cold expansion, the RTCE eliminates the need of different machines for predrilling and cold expansion. In addition, the misalignment between the predrilled hole and the cold expansion tool is almost eliminated which otherwise makes the plastic zone around hole non-axisymmetric and may even result angular deviation in residual stress up to 400% [8].

The simultaneous rotation and insertion of the tool along with minimum misalignment between the tool and the hole during the RTCE limits the angular deviation in compressive residual stress. In a separate study [16] it is found that due care during the RTCE may even restrict the angular deviation to less than 10%. In addition, significant improvement in the hardness of the inner surface of the hole

and a very good surface finish can be obtained. In turn the fatigue performance around the hole enhances.

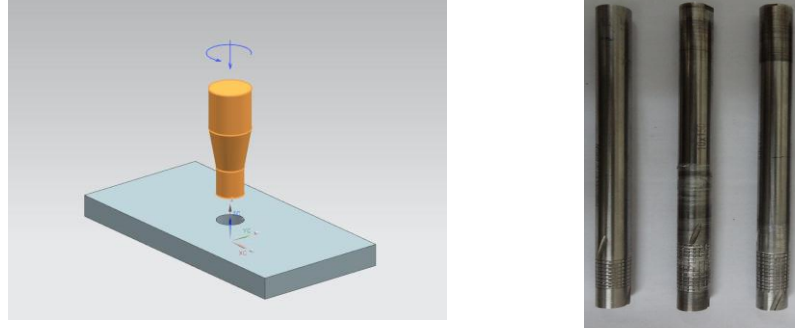


Figure 3: (a) RTCE process and (b) Three different tools of diameter 9.2, 9.5 and 9.9 mm

The cold expansion in RTCE process consist of three steps namely expansion, retention and recovery. In the expansion phase the tapered section passes through the entire thickness of the hole. In the retention phase the upper diameter passes through the plate thickness and reverts back at the same axial feed rate, RPM and the direction of rotation. The length of the tool passes through the hole in the retention phase is 3mm on the top of the plate thickness in order to ensure the bottom phase is also retained before the recovery starts. Subsequently when the tool reverts back and contact between tool and the hole is lost the recovery starts when some of the stress is relieved. The retention is the distinguish feature of the RTCE, helps in generating excessive compressive residual stress.

In the present study we have used three tapered tools with different bottom diameters (d_b) namely 9.2mm, 9.5mm and 9.9mm with same taper length of 15mm. The upper diameter (d_u) of all the three tools are kept at 10mm, equal to the final hole diameter, as shown in the figure 3(b). The diameters of the predrilled holes are kept same as the tool bottom diameter d_b . The edge of the tool at the bottom is chamfered to facilitate the initial entry of the tool followed by expansion of the hole through insertion of tapered section. The three cold expanded holes with final diameter of 10mm were produced with different degrees of cold expansion (DCE).

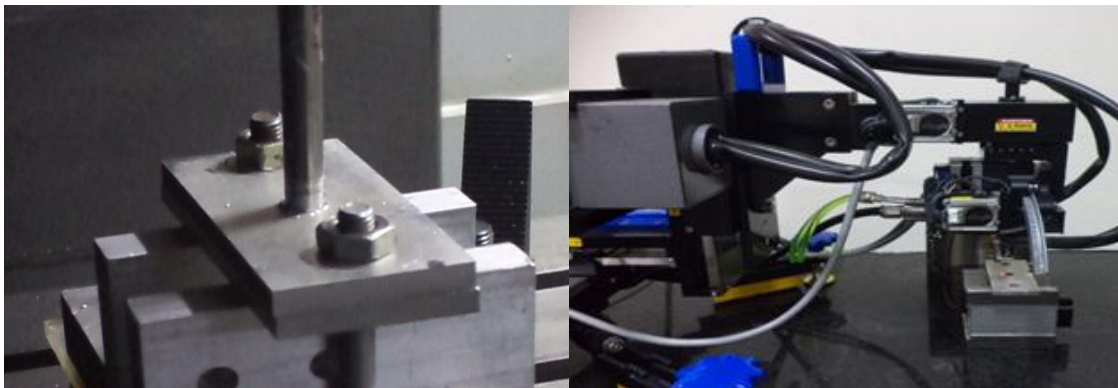
The degree of cold expansion is given by the following equation:

$$\% \text{ DCE} = \frac{d_u - d_b}{d_b} \times 100 \quad (1)$$

Based on the equation (1) the degree of cold expansion for 9.2, 9.5 and 9.9mm comes out to be 8.69, 5.26 and 1.01% respectively.

3.2 Experimental Setup

The rotating tool cold expansion hole process consists of a CNC milling machine, X-ray diffraction and Fatigue testing machine. In this experiment, hole is drilled into the work piece using drilling machine, a rotating tapered tool is inserted into the undersized hole using CNC milling machine as shown in figure 4(a). The forces acting in the process are measured using force sensor. The induced residual stresses are measured using X-ray diffraction, as shown in figure 4(b), on the top surface. ANSYS FEA simulation software is used to model the process.



(a)

(b)

Figure 4: Experimental Setup: (a) RTCE (b) XRD Measurement

The work piece material is commercial aluminium and the tool is high speed steel. The tool was fed at a constant rate of 8mm/min and the angular speed of the tool was kept at 60rpm. The work piece was mounted on Chrysler dynamometer and then lateral and axial forces inserted by the tool on the work piece were recorded during

the RTCE operation. The typical diagram showing the measured forces is given in figure (5).

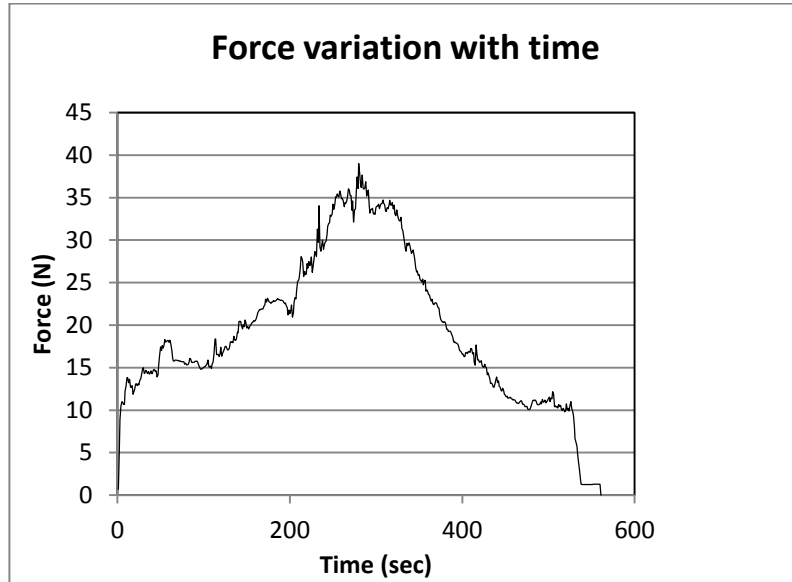


Figure 5: Force variation F_y with time, initial diameter 9.9mm

The induced residual stress on the surface was measured using X-ray diffraction technique. The measured residual stresses at various points situated at different distances from the hole for the foregoing cases of cold expansion and a predrilled hole are shown in figure (6).

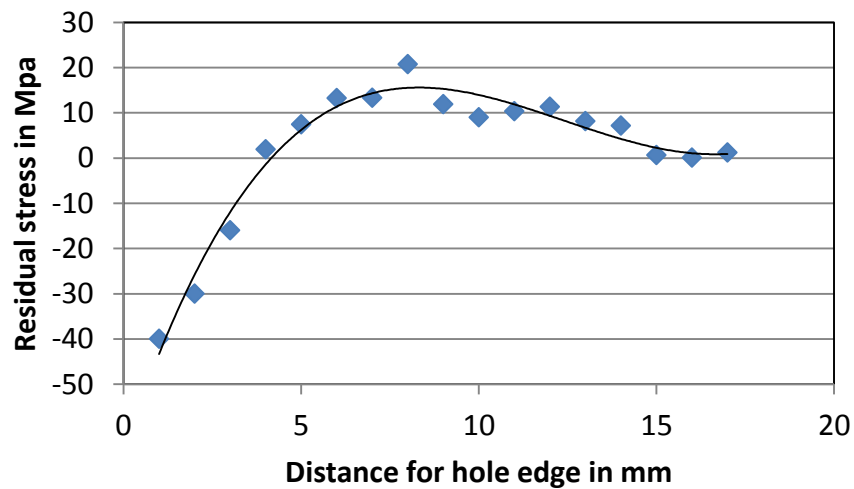


Figure 6: The residual stress variation for tool diameter 9.9mm

It can be seen that the RTCE has induced significant compressive residual stress in the vicinity of the hole. However, it is interesting to note that the maximum DCE 8.69% resulted in minimum compressive residual stress among the three cases. Moreover the moderate DCE resulted in maximum compressive residual stress is obtained with 5.26% DCE.

The RTCE process yields a worth mentioning difference in through thickness residual stress distribution. The conventional cold expansion techniques result in lesser compressive or even tensile residual stresses at the entrance face. The middle face may have up to three times more compressive residual stresses than the entrance face. In contrast, RTCE results in higher compressive residual stress at the entrance face than the exit face as shown in table (1).

Table 1: Maximum residual stress induced in the RTCE process near the hole for three different DCE

Tool diameters	9.2	9.5	9.9
Top surface	-41 MPa	-48 MPa	-40 MPa
Bottom surface	-24 MPa	-31 MPa	-18 MPa
Ratio	1.7	1.65	2.4

The tool remains in contact to the entrance face throughout the entire cold expansion in the RTCE. The retrieving tool retards the recovery process and even repairs the damage caused during the tool insertion face. In a way this is similar to the double expansion process where the cold expansion ball is re-entered from entry or the exit face. It has been evidenced that such re-entries are helpful in improving the fatigue life of the component by increasing the compressive residual stress at the entrance face. The experimental results make it imperative to comprehensively understand the mechanism of RTCE. Therefore a finite element based numerical study, is presented in the next chapter.

Chapter 4

Numerical Modeling

The mathematical models of the conventional cold expansion techniques are primarily based on structural analysis. In these models contact friction at tool-work piece interface has limited role as the cold expansion is carried out with lubricants leaving almost negligible possibility of surface alteration at micro-level. In the initial references on finite element based studies on cold expansion the effect of friction was ignored [23]. Subsequently the effect of friction with a small value of coefficient of friction has been considered. The friction has a distinct and major role in the RTCE process as the tool is expected to stir the surface and alter the surface properties. Most of the previous studies on conventional cold expansion are based on uniform displacement. The similar approach may not fully represent the RTCE, particularly the recovery stage after tool retrieval, due to temperature dependent non linearity. The RTCE process in the present work is simulated through coupled thermo-mechanical analysis incorporating the heat generation model and contact pressure model in the simulation as presented in the subsequent sections.

4.1. Heat generation model

The heat generation and material interaction at the tool and hole interface in the RTCE process appears similar to that between tool pin and the surrounding material in the friction stir welding. The analytical heat generation model of friction stir welding given by Schmidt [24] is apt for the RTCE process. The heat is generated by combined sliding and sticking. The sliding is the condition when the contact shear stress is smaller than the internal material yield shear stress. In turn the material at the interface shears slightly to a stationary elastic deformation where the shear stress equals the ‘dynamic’ contact shear stress. Based on Coulomb’s friction

law the critical friction stress ($\tau_{\text{contact, sliding}}$) required for a sliding condition is given as follows

$$\tau_{\text{contact,sliding}} = \mu p = \mu \sigma_y \quad (2)$$

where μ is coefficient of friction at the tool-work piece interface, p is the normal pressure exerted by the tool on the surface and σ_y is the yield stress.

On the other hand sticking is the condition when the contact shear stress exceeds yield shear stress, the material at the interface accelerates along with the tool till its velocity becomes equal to the tool tangential velocity. The material at the far away stationary points and those moving with the tool counter balance the velocity difference by plastic deformation. The upper limit formulation allows the shear stress responsible for deformation to be independent of the width of the deformation zone and to be treated as a shear surface [24]. This condition can be treated as uniaxial tension and pure shear. Thus the contact shear in the sticking condition can be obtained by equating with the von-mises yield criterion in the same condition, as follows:

$$\tau_{(\text{contact,sticking})} = \tau_{\text{yield}} = \frac{\sigma_y}{\sqrt{3}} \quad (3)$$

The heat generation over an elemental area dA due to sliding and sticking friction can be given by equation 4 and 5 as follows

$$d\dot{Q}_{\text{sliding}} = \mu \sigma_y \times dA \times r\omega \quad (4)$$

and

$$d\dot{Q}_{\text{sticking}} = \frac{\sigma_y}{\sqrt{3}} \times dA \times r\omega \quad (5)$$

In actual practice more often the processes like FSW are governed by partial sliding/sticking condition. The material surrounding the tool attains a velocity less than the tool surface velocity. In this condition the contact shear stress equals to the yield shear stress due to quasi-stationary plastic deformation rate [24]. In the absence of mechanism to estimate the extent of contribution of sliding and sticking friction, weighting function is used. The dimensionless slip rate δ , which relates the velocity of the contact point at the material surface relative to the tool point in contact [24] is used as weighting function parameter. Using the δ the total heat generation rate is given as follows.

$$d\dot{Q}_{\text{Total}} = (1 - \delta)d\dot{Q}_{\text{sliding}} + \delta d\dot{Q}_{\text{sticking}} \quad (6)$$

$$d\dot{Q}_{\text{Total}} = (1 - \delta)\mu\sigma_y \times dA \times r\omega + \delta \frac{\sigma_y}{\sqrt{3}} \times dA \times r\omega \quad (7)$$

Thus the heat flux rate (\dot{q}) can be given by the following equation.

$$\dot{q} = (1 - \delta)\mu\sigma_y(T) \times r\omega + \delta \frac{\sigma_y(T)}{\sqrt{3}} \times r\omega \quad (8)$$

It is to be noted that the yield stress in equation (8) is temperature dependent. A friction coefficient μ is assumed to be temperature independent as it is found that the range of temperature generated at the interface (experimentally measured) is not sufficient but is in adequate to alter the value of μ [25]. Moreover, due to partial sliding and sticking conditions, predetermining of coefficient of friction is not possible. In addition the previous investigation has shown that the friction coefficient between aluminium and steel changes with the normal stresses [26]. Thus, unlike the previous investigation considering a predetermined value, the coefficient of friction in this investigation is considered as a state variable and arrived through simulation as presented shortly. Similarly the dimensionless slip rate δ is also arrived through simulation. A proper combination of μ and δ should result

in agreement between actual and simulated residual stresses. The simulation procedure is presented in section 4.4.

4.2 Tool Motion

As the tool is inserted into the undersized hole with a specified feed rate, the contact of the tool with the work piece varies with time. It is important to analyze the contact of the tool with work piece at different instants of time because it gives an indication of a change of pressure on the surface area at different times. Feed rate of the tool is 8mm/min and instant of the contact is calculated based on time (distance travelled by the tool/feed rate). Based on the tool design the bottom cylindrical portion having 10mm length travels for 75 seconds and the tapered portion starts at this instant. The figure (7) shows the diagram of tool contact with work piece at different instants of time.

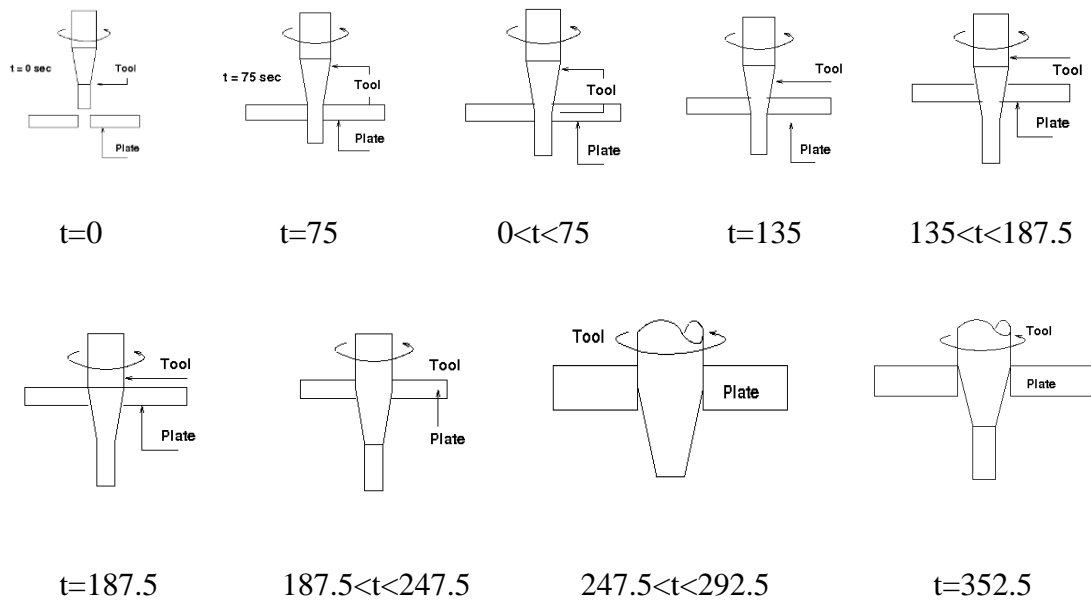


Figure 7: Tool position at different times in sec. during RTCE process

The pressure exerted by the tool on the internal hole surface of the work piece varies due to the variation of tool geometry at the interface. Force exerted by a tool on the work piece at each instant of time is measured using Kistler dynamometer. Area of contact at different instants of time is calculated as shown in the table (2).

Table 2: Area of contact at different instants of time

Time(sec)	Area of contact at different instants	x
0-75	$A = \pi D_i x$	$x = f \times t$
75-135	$A = \pi \left[\left(D_i + \frac{(10 - D_i)x}{30} \right) x + D_i(8 - x) \right]$	$x = f \times (t - 75)$
135-187.5	$A = \pi 8 \left[10 + \frac{(10 - D_i)x}{15} \right]$	$x = f \times (t - 135)$
187.5-247.5	$A = \pi \left[10x + \left(10 - \frac{(10 - D_i)(8 - x)}{30} \right) (8 - x) \right]$	$x = f \times (t - 187.5)$
247.5-292.5	$A = 80\pi$	-
292.5-352.5	$A = 10\pi x$	$x = f \times (352.5 - t)$

where D_i is the diameter of the pre drilled hole, f is the feed rate and t is the time.

4.3 Contact Pressure Model

The tool and the hole contact in the RTCE process is unlike the other cold expansion technique due to retention and retrieval of the tool, as described in the previous section. The contact area during the tool insertion phase continuously increases followed by a constant contact area in the retention phase. When the tool reverts the contact area again decreases till the no contact is reached. In order to understand the RTCE process the present numerical model takes into account the actual pressure exerted by a tool on the hole surface. The contact pressure is calculated for staggered layers taking into account the measured force and the calculated area of contact. A representative contact pressure for the top layer of thickness 1mm is shown in the figure (8). It can be seen that the initial contact pressure is quite high followed by a stagnant regime. While reverting, the tool contact reduces and in turn the pressure increases that reaches to peak before the tool loses contact. This positively affects the compressive residual stress specifically on the top most layer as seen in the foregoing section. Unlike the previous studies, in the present model the transient contact pressure is used as a boundary condition in structural analysis. The simulation of the RTCE process using the heat source and contact pressure models is presented in the following section.

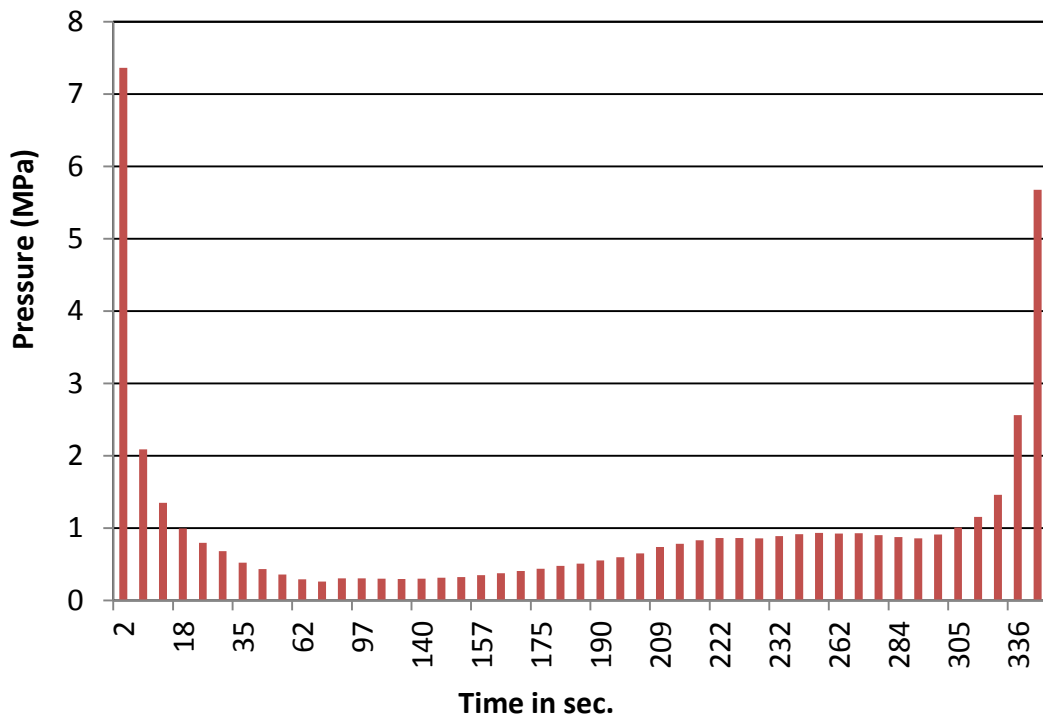


Figure 8: Pressure variation with time for tool diameter 9.5 mm

4.4 Simulation

The thermo-mechanical simulation of RTCE process is carried out using ANSYS APDL. The thermal analysis is carried out and then it is switched to structural analysis giving temperature boundary conditions generated during thermal analysis. The residual stresses measured after RTCE process using X-ray diffraction are on the top surface of the workpiece. The actual thickness of the work piece is 8mm but in modelling only top portion 1mm is considered to save simulation time. The dimension of the model is 100x50x1 mm assuming the work-piece is discretized into 1mm each having an impact with the tool.

The mesh is comprised of a total number of 13864 elements. The half section of the 3D model is considered and its mesh is as shown in figure (9) due to symmetry. The element used is solid 70 in thermal analysis which is convertible to an equivalent solid 185 element in structural analysis. Solid70 has a three-dimensional thermal conduction capability and solid185 is used for the three-dimensional modeling of solid structures.

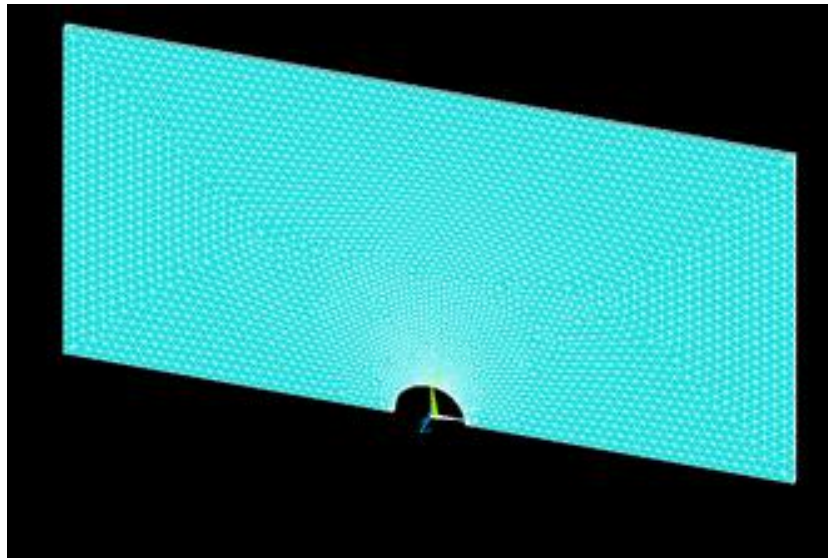


Figure 9: A half section symmetrical 3 D model

The material used is nonlinear isotropic hardening. As in this process there is an observation of temperature rise with time so, the temperature dependent material properties are considered. The stress-strain curve of pure aluminium [27] for different temperatures are shown in figure (10).

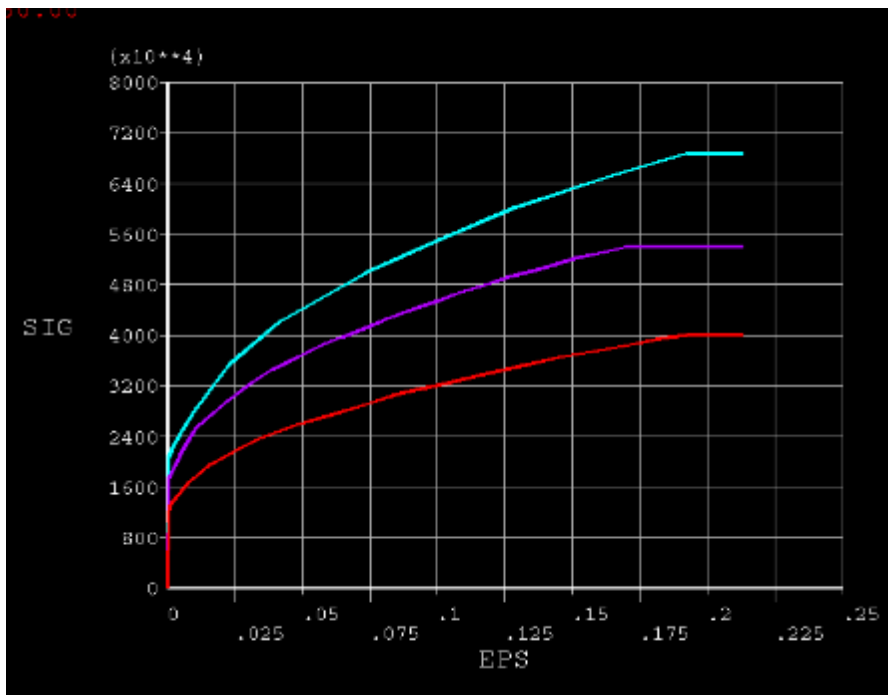


Figure 10: Stress Strain curve of pure aluminum at different temperatures

The thermal and the structural loads are applied on staggered layers. Firstly in the model development stage different values of the friction coefficient μ and the dimensionless slip rate δ are applied for simulating the cold expansion of the hole with initial diameter 9.5mm. Subsequently the combination of μ and δ giving the minimum difference in between the experimental and simulated residual stress at the top most layer results are applied for the other hole diameter namely 9.2 and 9.9mm for the purpose of validation.

In the thermal analysis heat flux is applied for the time as long as the tool remains in contact and subsequently the internal hole surface is allowed to cool by convection. The topmost layer remains in contact with the tool for maximum time (around 350 seconds). In the structural analysis the contact pressure is applied for the same duration as in the thermal analysis and subsequently the internal surface is allowed to recover. The half section model is considered due to symmetry. The representative tangential residual stress profiles are given in figure (11). The calculated residual stress at the top surface for 9.5mm initial diameter case and the error in the prediction is shown in table (3).

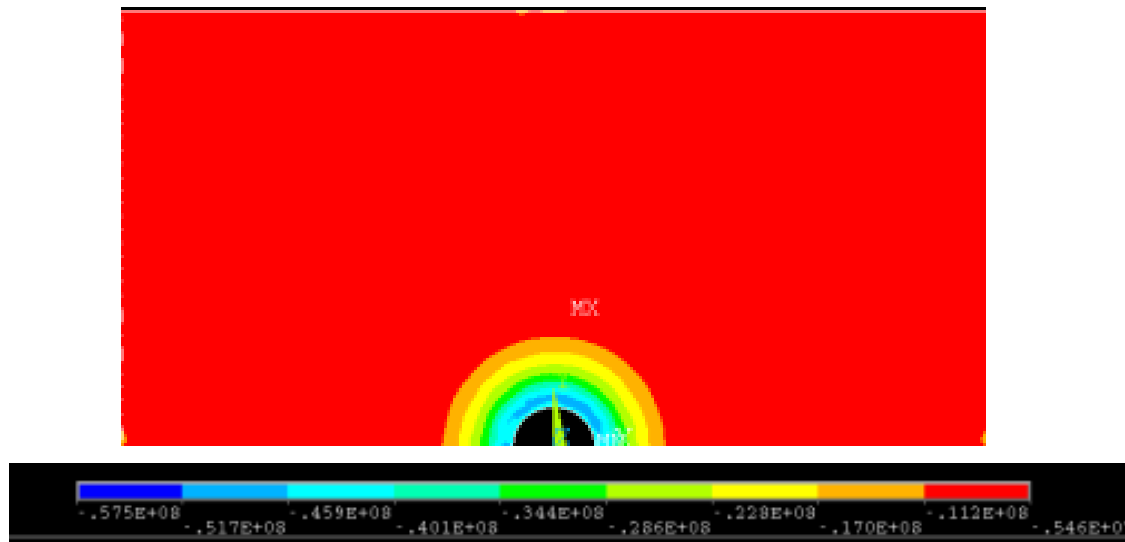


Figure 11: Tangential residual stress profile for 9.5 tool $\mu=0.1$ $\delta=0.5$

Table 3: Error in predicted residual stress at different δ and μ with tool diameter 9.5 mm

Tool initial diameter - 9.5mm	$\delta \backslash \mu$	0.1	0.25	0.5	0.75	1
		0	29.25	2.98	0.72	
	0.25		0.27	0.1	0.95	
	0.5	1.23	1.52	0.9		2.49
	1	31.28	31.28	31.28		31.28

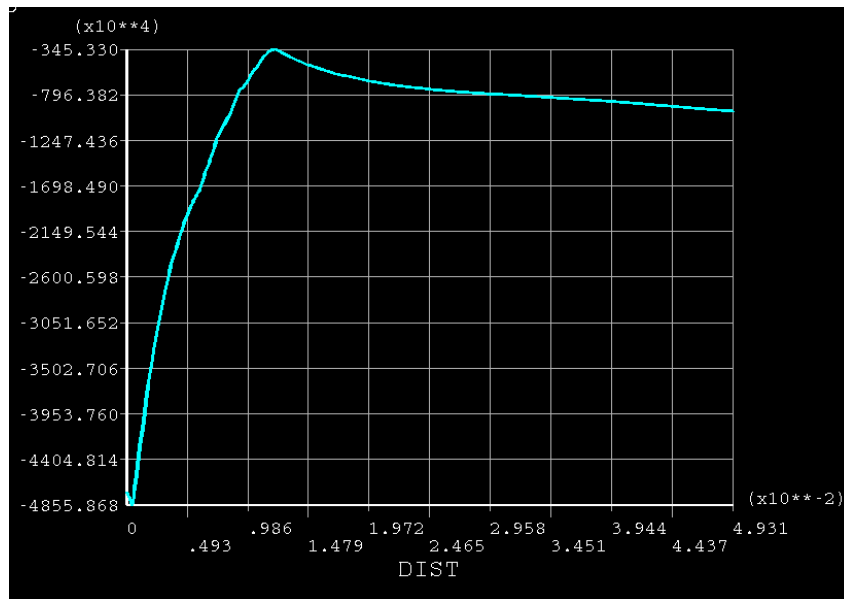
It can be seen that at $\delta = 0.25$ the predicted residual stress is very near to the experimental residual stress within 2% of error. When the same value of δ is used for simulating the residual stresses in 9.9 and 9.2mm initial hole diameter, the error was limited to 4.2 % and 5.9% respectively. It is imperative that the model is capable to represent the rotating tool cold expansion. In the subsequent chapter more results have been presented and discussed in detail to understand the underlying mechanism of RTCE.

Chapter 5

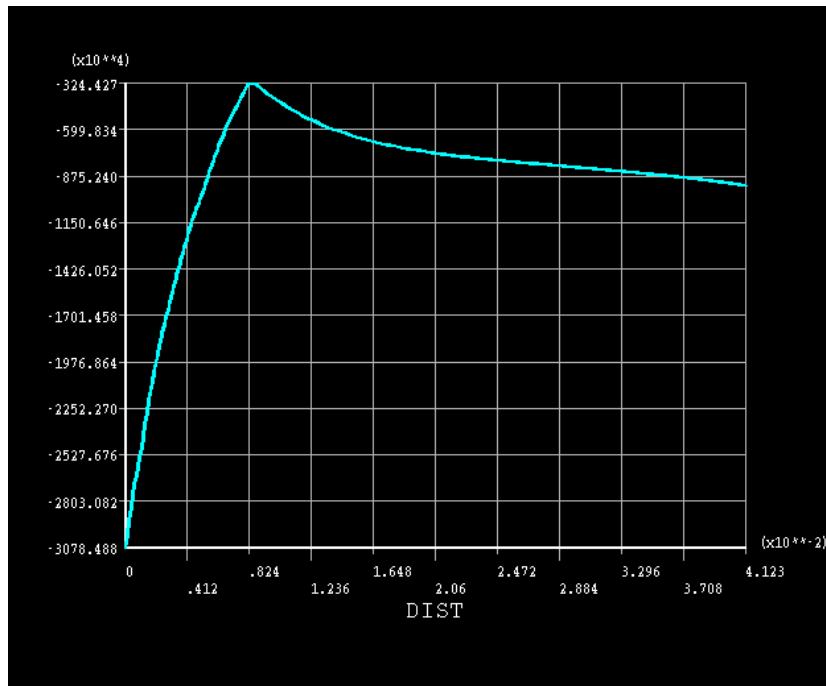
Results and Discussion

5.1 Variation of Residual stress through thickness:

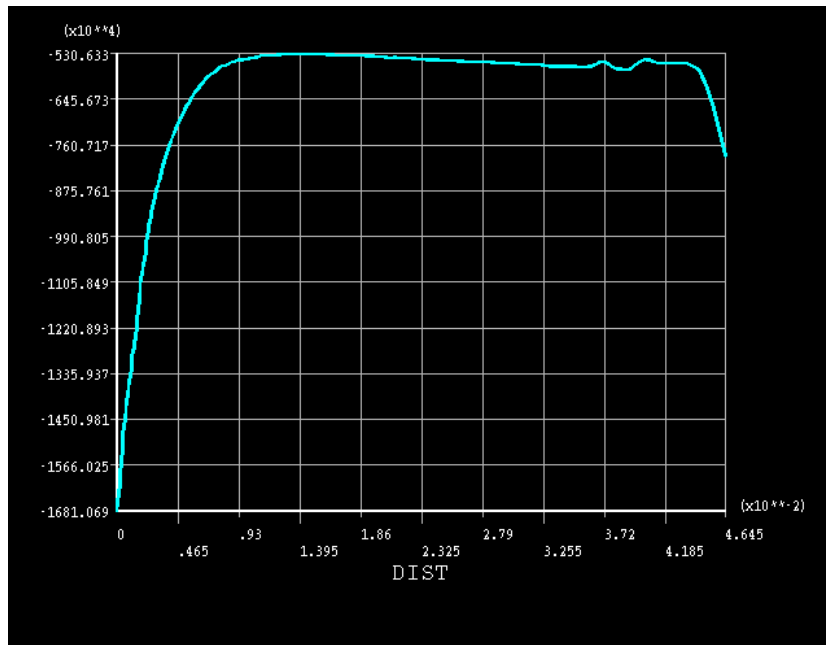
In conventional cold expansion techniques the residual stress at the topmost and intermediate layers are found to be minimum and maximum respectively. The simulation results of RTCE indicate that the residual stress continuously decreases from top to bottom surface. The residual stress at top, middle and bottom plane for 9.5mm initial hole diameter are shown in figure (12).



(a) Top Section – Maximum compressive residual stress -48.55MPa



(b) Middle section- Maximum compressive residual stress -30.78MPa



(c) Bottom section- Maximum compressive residual stress -16.81MPa

Figure 12: Simulation results at different sections, tool initial diameter 9.5 mm

It can be seen that the top layer has the maximum and the bottom layer has the minimum compressive residual stress. Unlike the conventional cold expansion

process RTCE prevents the top layer (entry face) damage, though the bottom layer compressive residual stresses are invariably found lesser irrespective of the degree of cold expansion as shown in the figure (13) depicting the experimental stress values at top and bottom surfaces. It is to be noted that both the layers passes through retention face and unlike the conventional techniques, the exit damage is not responsible for lesser stress at the bottom surface.

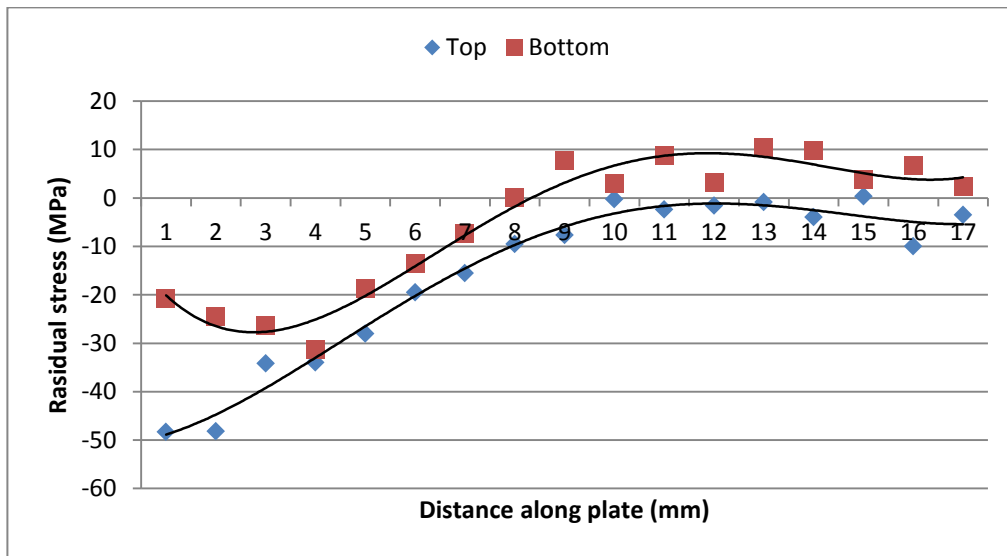


Figure 13: Experimental results at top and bottom plane of the work piece, processed with 9.5 mm tool

The RTCE process conditions and the tool geometry can be altered to bring positive impact on bottom surface residual stress. Many more experiments are required to understand the inter-relation between the tool geometry (tapered length and retention length, tool motion, tool feed rate and rpm) and DCE. The present study brings out the fundamental understanding of RTCE process and explains the roles of coefficient of friction and dimensionless slip rate, as described in the following section.

5.2 At the role of μ and δ :

It is evident from the foregoing discussion that dimensionless slip rate δ is an important state variable that depicts the RTCE process. The operating conditions of

the present work is well represented by $\delta = 0.25$. This indicates the role of plastic deformation in the RTCE. A significant amount of energy is used in plastically deforming the tool work piece interface. However, the plastic deformation only up to a limit of DCE is useful in the cold expansion. It can be seen that with moderate DCE (9.5mm hole diameter) more compressive stress is produced than the other two hole diameters namely 9.2mm and 9.9mm. This result is in agreement with the existing experimental evidences on conventional cold expansion. A moderate DCE ranging between 4-6% produces optimal compressive residual stresses as seen in figure (14). The lower DCE doesn't provide sufficient compression while too high degree of cold expansion permanently damages the hole and relieves the residual stress.

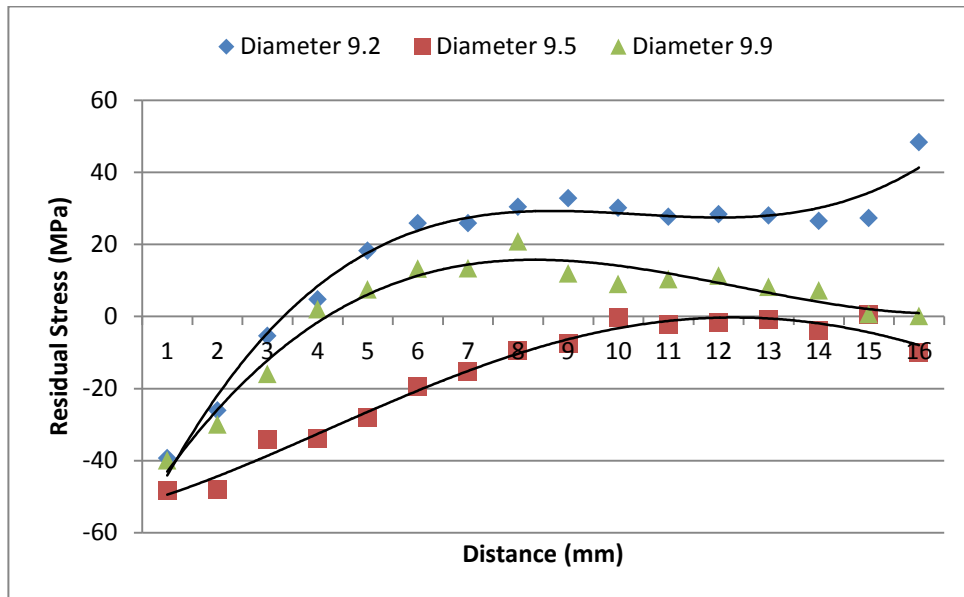
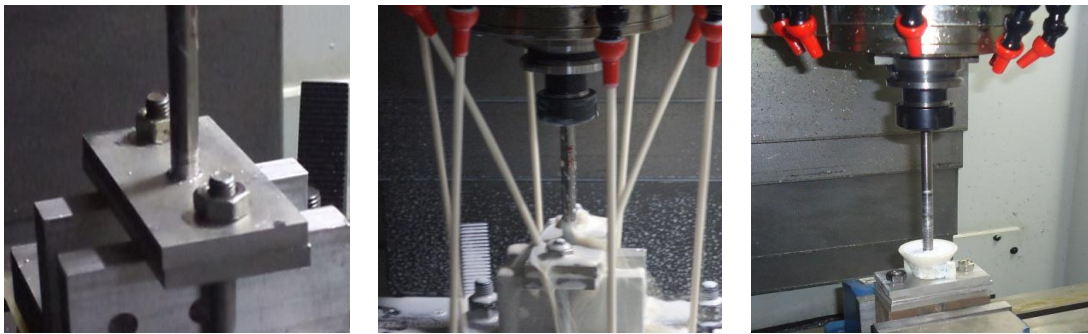


Figure 14: Residual stress variation with different tools

The numerical results could not reflect much on the role of coefficient of friction. In order to understand the effect of friction few more additional experiments were carried out aiming at generating different friction conditions at the tool work piece interface. These conditions referred as wet and abrasive conditions in the forthcoming discussion have been achieved through introduction of water soluble oil and abrasive material respectively during the RTCE. The original RTCE without any external medium is referred as dry condition.

The wet RTCE was conducted in flooded condition similar to the metal cutting operation where the tool and the work piece are flooded with synthetic or mineral oil. This arrangement is expected to lubricate the tool work piece interface and simultaneously cool down the work piece. Suitable water-soluble metal cutting oil is used in the present investigation. In the abrasive RTCE nano-sized alumina powder was fed along with the tool into the hole using a funnel. The abrasive particles are expected to increase the friction between the tool and the work piece. Figure (15) shows all these arrangements.



Dry condition

Wet condition

Nano-powdered condition

Figure 15: Experimental setup showing three different conditions

The maximum compressive residual stress on the top of the surface with varying DCE under three different, dry, wet and abrasive, conditions are compared in figure (16). As mentioned earlier the dry condition follows the reported results however, the residual stresses' trend with wet and abrasive conditions are mutually opposite as well as contrary to the foregoing expected trend. It is interesting to note that abrasive RTCE produces more compressive residual stress at higher DCE. It is even marginally higher than that produced with dry medium at the same DCE. On the contrary the compressive residual stress under the lubricating and cooling effect imposed by the water soluble under the wet condition is maximum at the minimum DCE. It seems that the excessive friction due to the abrasive particles softens the material and avoids the damage caused at higher DCE that appears with the dry condition. On the other hand, the residual stress under the wet condition is

maximum at the minimum DCE. At minimum DCE residual stresses under wet and abrasive conditions matches with each other however at higher DCE the residual stress drastically reduces. It can be inferred that at lower DCE both the fluid and solid particles act as lubricant and yield similar effects. However, increment in DCE with abrasive condition results in more frictional heat that allows softening of material and the tool passes through hole and reverts back without damaging the surface. This may lead to higher compressive residual stress at higher DCE under the abrasive conditions. On the other hand, the wet RTCE at higher DCE in the absence of sufficient friction works more like a drill bit and removes the material in place of compressing it in the lateral directions.

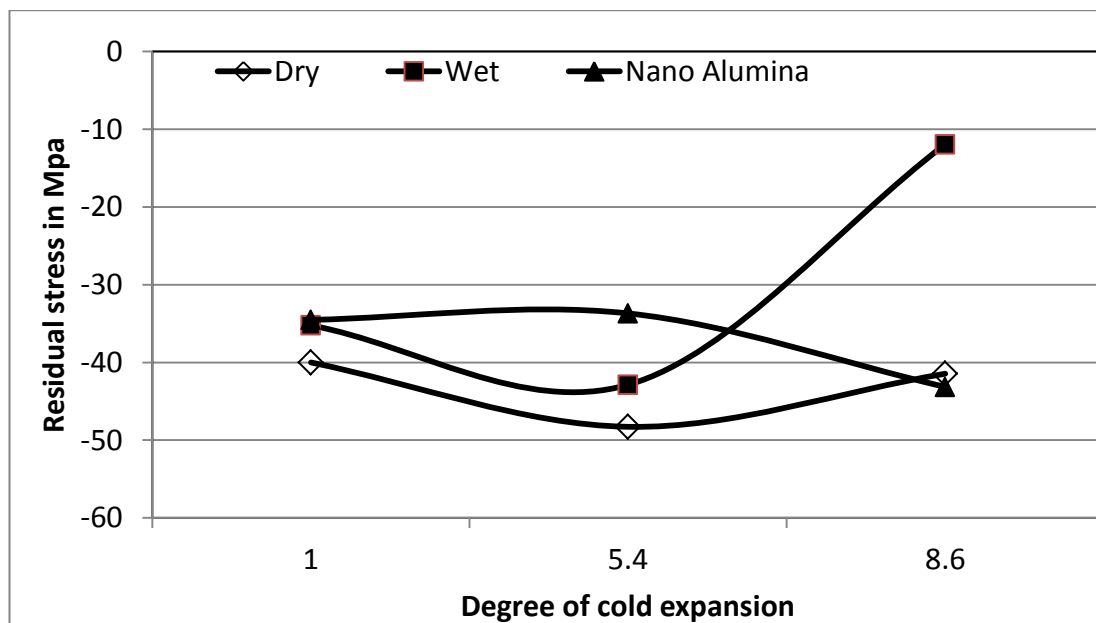


Figure 16: Maximum compressive residual stress under three different conditions for all DCE

The simulation is conducted for different values of μ and δ , as these are the important parameters in RTCE process. The obtained results are validated with the experimental results. The percentage error is least for $\mu=0.25$ and $\delta=0$ for tool 9.2, $\mu=0.5$ and $\delta=0.25$ for tool 9.5 and $\mu=0.5$ and $\delta=0.25$ for tool 9.9 respectively. Table (4) and table (5) shows the maximum residual stress values for all parameters and percentage error when compared with experimental results respectively.

Table 4: Results showing the maximum residual stress when compared to experimental value

	Max Compressive Stress in MPa					Experimental Results in MPa
Tool = 9.2	$\mu=0.1$	$\mu=0.25$	$\mu=0.5$	$\mu=0.75$	$\mu=1$	
$\delta=0$	-43.6	-39.96	-19	-42.4	-19.18	-39.35
$\delta=0.25$		-41.71	-43.21	-19.6		
$\delta=0.5$	-42.58	14.32	-48.78	-44.7	-8.79	
$\delta=1$	-47.92	-47.92	-47.92		-47.92	
Tool=9.5	$\mu=0.1$	$\mu=0.25$	$\mu=.5$	$\mu=0.75$	$\mu=1$	
$\delta=0$	-19.03	-45.3	-49	-48.41	-50.44	-48.28
$\delta=0.25$		-48.55	-48.38	-49.23		
$\delta=0.5$	-49.51	-49.8	-49.18	-50.3	-50.77	
$\delta=1$	-17	-17	-17		-17	
Tool 9.9	$\mu=0.1$	$\mu=0.25$	$\mu=0.5$	$\mu=0.75$	$\mu=1$	
$\delta=0$	-34.6	-36.63	-42.35	-38.94	-40.95	-40
$\delta=0.25$		-38.31	-40.12	-41.04		
$\delta=0.5$	-51.28	-41.3	-22.75	-42.68	-43.17	
$\delta=1$	-45	-45	-45	-45	-45	

Table 5: Error in predicted residual stress at different δ and μ

Tool 9.2		$\mu=0.1$	$\mu=0.25$	$\mu=0.5$	$\mu=0.75$	$\mu=1$
	$\delta=0$	4.25	0.61	20.35		20.17
	$\delta=0.25$		2.36	3.86	19.75	
	$\delta=0.5$	3.23	53.67	9.43		30.56
	$\delta=1$	8.57	8.57	8.57		8.57
Tool 9.5		$\mu=0.1$	$\mu=0.25$	$\mu=0.5$	$\mu=0.75$	$\mu=1$
	$\delta=0$	29.25	2.98	0.72		2.16
	$\delta=0.25$		0.27	0.1	0.95	
	$\delta=0.5$	1.23	1.52	0.9		2.49
	$\delta=1$	31.28	31.28	31.28		31.28
Tool 9.9		$\mu=0.1$	$\mu=0.25$	$\mu=0.5$	$\mu=0.75$	$\mu=1$
	$\delta=0$	5.4	3.37	2.35		0.95
	$\delta=0.25$		1.69	0.12	1.04	
	$\delta=0.5$	11.28	1.3	17.25		3.17
	$\delta=1$	5	5	5		5

Chapter 6

Conclusion

The numerical and experimental study of RTCE is concluded with the following remarks

- It is feasible to achieve a significant amount of cold expansion through rotating tool cold expansion process.
- The Effectiveness of the developed process depends upon degree of cold expansion. Compared to the degree of cold expansion through conventional techniques (upto 4%) the proposed technique is capable to produce good results up to 8.69% of cold expansion.
- The numerical results indicate that the role of heat generated through friction and plastic deformation is critical to attain the best possible result. A synergy between the both yields the optimal results
- The developed approach would be useful in understanding the material behaviour in similar process like FSW/FSP.

Scope of future work

Further study can be made by changing the process parameters like feed rate and RPM to understand their relation with the process. The surface texture study can be made to further understand the behaviour. A separate study on compositing of layer during the RTCE is possible with some alteration in the proposed process. The cold expansion results can further be evaluated for the hardness of the surface and fatigue life.

References

- [1] Chakherlou, T. N. and Vogwell, J. (2003) The effect of cold expansion on improving the fatigue life of fastener holes. *Engineering Failure Analysis*. 10, 13–24.
- [2] Leon, A. (1998) Benefits of split mandrel cold working. *International journal of Fatigue*. 20(1), 1-8.
- [3] Maximov, J.T., Kuzmanov, T.V., Anchev, A.P. and Ichkova, M.D. (2006) A finite element simulation of the spherical mandrelling process of holes with cracks. *Journal of Materials Processing Technology*. 171, 459–466.
- [4] Mishra, R.S. and Ma, Z.Y. (2005) Friction stir welding and processing. *Materials Science and Engineering*. 50, 1–78.
- [5] Hossein Bisadi and Asghar Abasi. (2011) Fabrication of Al7075/TiB₂ Surface Composite Via Friction Stir Processing. *American Journal of Materials Science*. 1(2), 67-70.
- [6] Sharma, S.R., Ma, Z.Y. and Mishra, R.S. (2004) Effect of friction stir processing on fatigue behavior of A356 alloy. *Scripta Materialia*. 51, 237–241.
- [7] Kliman, V., Bily, M. and Prohacka, J. (1993) Improvement of fatigue performance by cold hole expansion. *International Journal of Fatigue*. 15(2), 101-107.
- [8] Liu, J., Shao, X.J., Liu, Y.S. and Yue, Z.F. (2008) Effect of cold expansion on fatigue performance of open holes. *Materials science and engineering*. A 477, 271-276.
- [9] Chakherlou, T. N. and Vogwell, J. (2004) A novel method of cold expansion which creates near-uniform compressive tangential residual stress around a fastener hole. *Fatigue and Fracture of Engineering Materials & Structures*. 27 (5), 343-351.
- [10] de Matos, P.F.P., Moreira, P.M.G.P., Pina, J.C.P., Dias, A.M. and de Castro, P.M.S.T. (2004) Residual stress effect on fatigue striation spacing in a cold-worked rivet hole. *Theoretical and Applied Fracture Mechanics*. 42, 139–148.

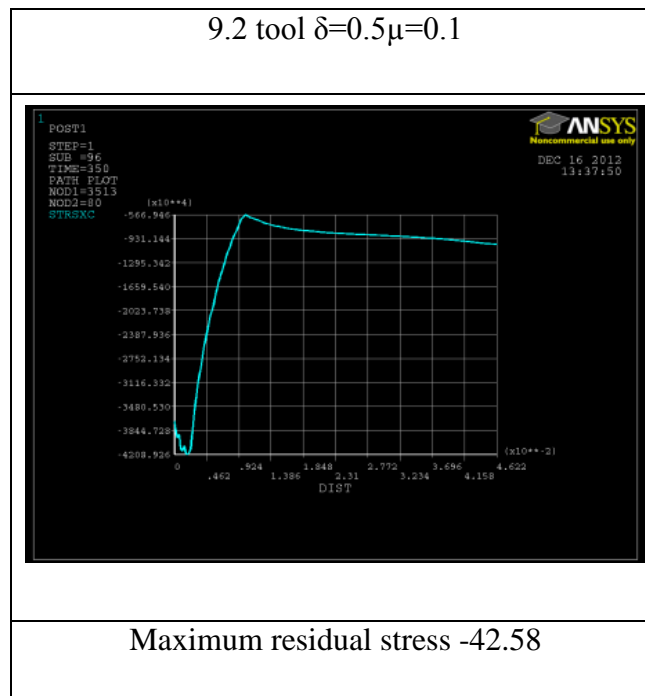
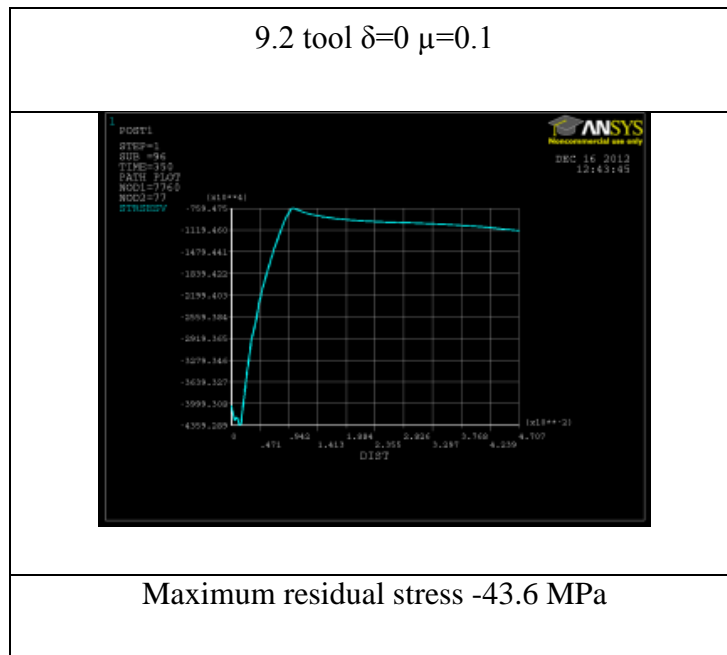
- [11] Jang, J. S. and Kim, D. W. (2008) Re-cold expansion process simulation to impart the residual stresses around fastener holes in 6061 A-T6 aluminium alloy. *Journal of engineering manufacture*. 222(11), 1325-1332.
- [12] Ni, D.R., Wang, D., Feng, A.H., Yao, G. and Ma, Z.Y. (2009) Enhancing the high-cycle fatigue strength of Mg-9Al-1Zn casting by friction stir processing. *Scripta Materialia*. 61, 568-571.
- [13] Arifvianto, B., Suyitno and Mahardika, M. (2012) Effects of surface mechanical attrition treatment (SMAT) on a rough surface of AISI 316L stainless steel. *Applied Surface Science*. 258, 4538-4543.
- [14] Jordan Maximov, T. and Galya Duncheva, V. (2008) A new 3D finite element model of the spherical mandrelling process. *Finite Elements in Analysis and Design*. 44, 372-380.
- [15] Shamdani, A. H. and Khoddam, S. (14 March 2012) A comparative numerical study of combined cold expansion and local torsion on fastener holes. *Fatigue and fracture of engineering materials and structures*. 35, 918-928.
- [16] Nitin Panaskar and Abhay Sharma. (working paper 2012-2013) Novel concept of combined cold expansion and nano-composite surface layering of fastener holes using rotating tool. IIT Hyderabad.
- [17] Chakherlou, T. N. and Yaghoobi, A. (2010) Numerical simulation of residual stress relaxation around a cold-expanded fastener hole under longitudinal cyclic loading using different kinematic hardening models. *Fatigue and Fracture of Engineering Materials & Structures*. 33(11), 740-751.
- [18] Aghdama, A.B., Chakherlou, T.N. and Saeedi, K. (2010) An FE analysis for assessing the effect of short-term exposure to elevated temperature on residual stresses around cold expanded fastener holes in aluminum alloy 7075-T6. 31(1), 500-507.
- [19] Amrouche, A., Su, M. and Mesmacque, G. (2008) Numerical study of the optimum degree of cold expansion: application for the pre-cracked specimen with the expanded hole at the crack tip. *Journal of material processing technology*. 197, 250-254.

- [20] Su, M., Amrouche, A., Mesmacque, G. and Benseddiq, N. (2008) Numerical study of double cold expansion of the hole at crack tip and the influence on the residual stresses field. *Computational Materials Science*. 41(3), 350- 355.
- [21] Houghton, S. J. and Campbell, S. K. (2011) Identifying the residual stress field developed by hole cold expansion using finite element analysis. *Fatigue & Fracture of Engineering Materials & Structures*. 35, 74-83.
- [22] Mahendra Babu, N.C., Jagadish, T., Ramachandra, K. and Sridhara, S.N. (2008) A simplified 3-D finite element simulation of cold expansion of a circular hole to capture through thickness variation of residual stresses. *Engineering Failure Analysis*. 15(4), 339–348.
- [23] Heller, M., Jones, R. and Williams, J.F. (1991) Analysis of cold-expansion for cracked and uncracked fastener holes. *Engineering Fracture Mechanics*.39(2), 195-212.
- [24] Schmidt, H., Hattel, J. and Wert, J. (2004) An analytical model for the heat generation in friction stir welding. *Modelling and simulation in materials science and engineering*. 12, 143–157.
- [25] Bansal P. and Mandal N. R. (2011) Effect of Tool Geometries on Thermal History of FSW of AA1100. *Supplement to the welding Journal*. 90, 129-134.
- [26] Javadi, M. and Tajdari, M. (2006) Experimental investigation of the friction coefficient between aluminium and steel. *Materials Science-Poland*, 24(2/1), 305-310.
- [27] Nguyen Chinh, Q., Judit Illy, Zenji Horita and Terence Langdon, G. (2005) Using the stress–strain relationships to propose regions of low and high temperature plastic deformation in aluminum. *Materials Science and Engineering*. A 410–411, 234–238.

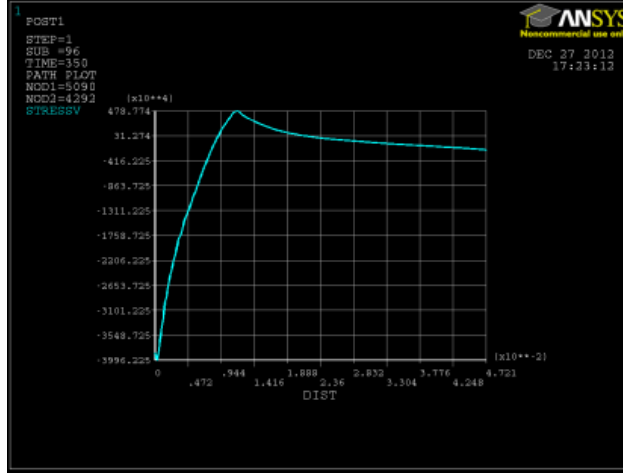
Appendix

Simulation results showing tangential stress variation for different parameters of all tools.

Results of Tool diameter 9.2:

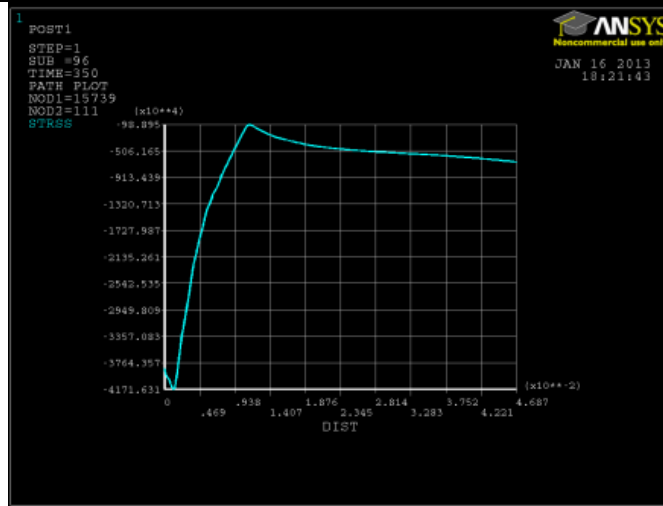


9.2 tool $\delta=0$ $\mu=0.25$



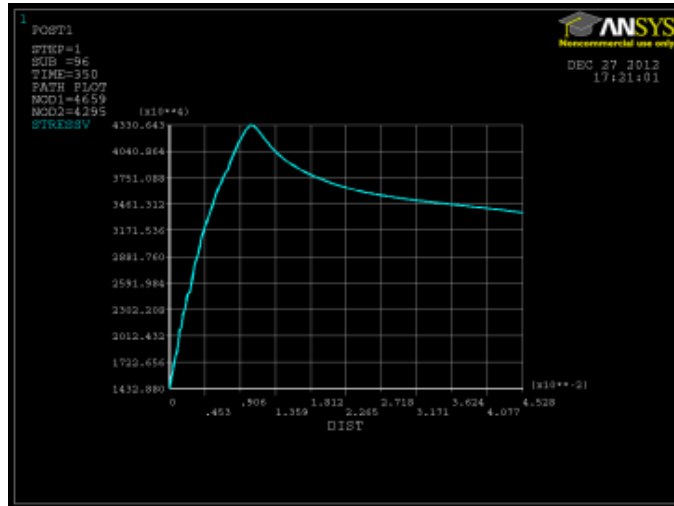
Maximum residual stress -39.96

9.2 tool $\delta=0.25$ $\mu=0.25$



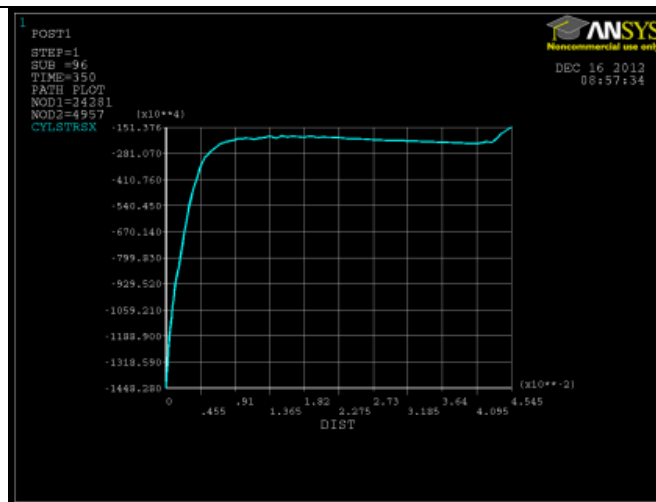
Maximum residual stress -41.71Mpa

9.2 tool $\delta=0.5\mu=0.25$



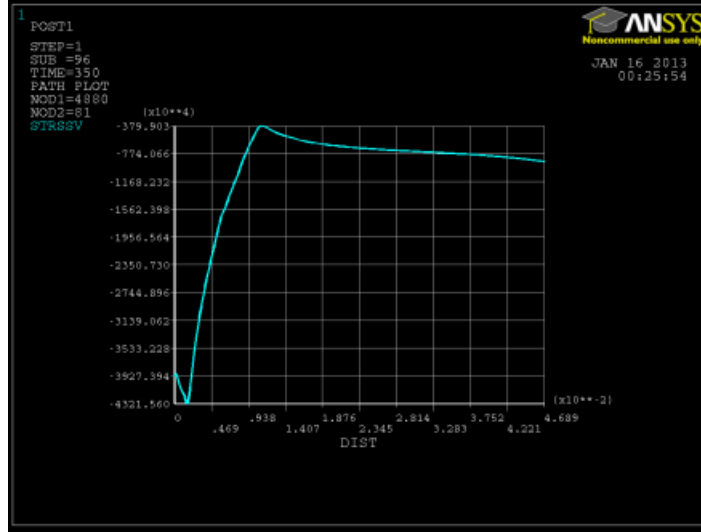
Maximum residual stress- -14.32

9.2 tool $\mu=0.5\delta=0$



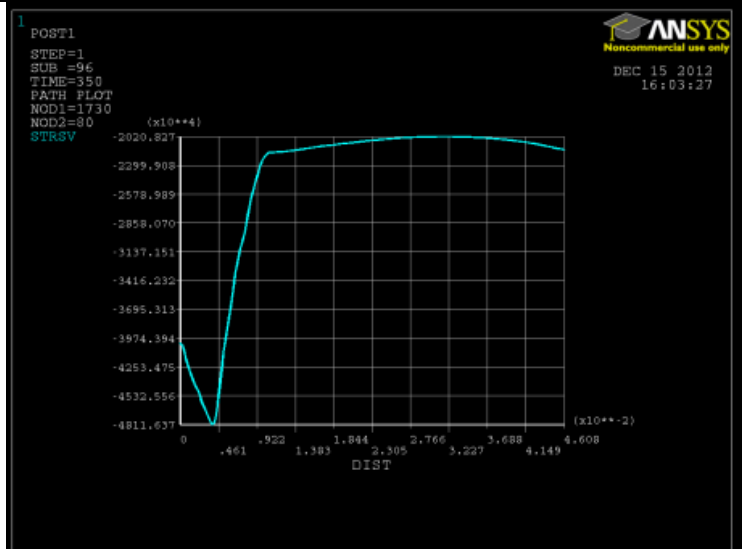
Maximum residual stress -19MPa

9.2 tool $\mu=0.5\delta=0.25$



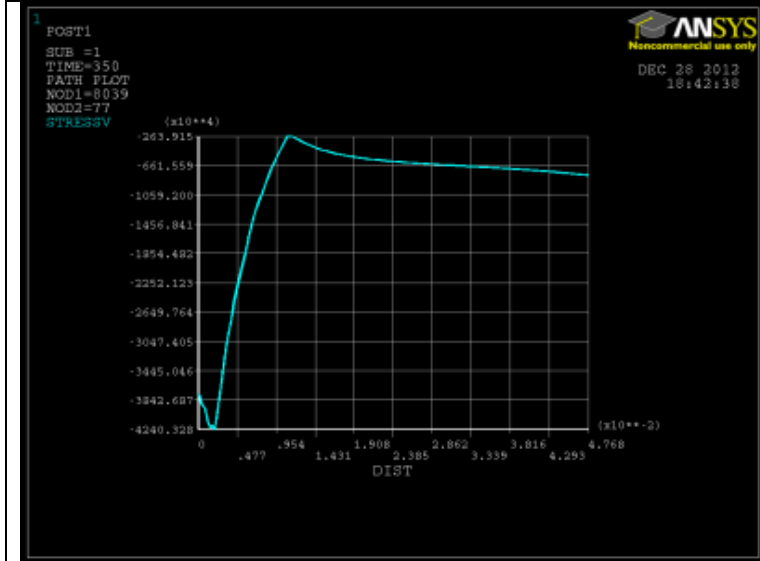
Maximum residual stress- -43.21

9.2 tool $\mu=0.5\delta=0.5$



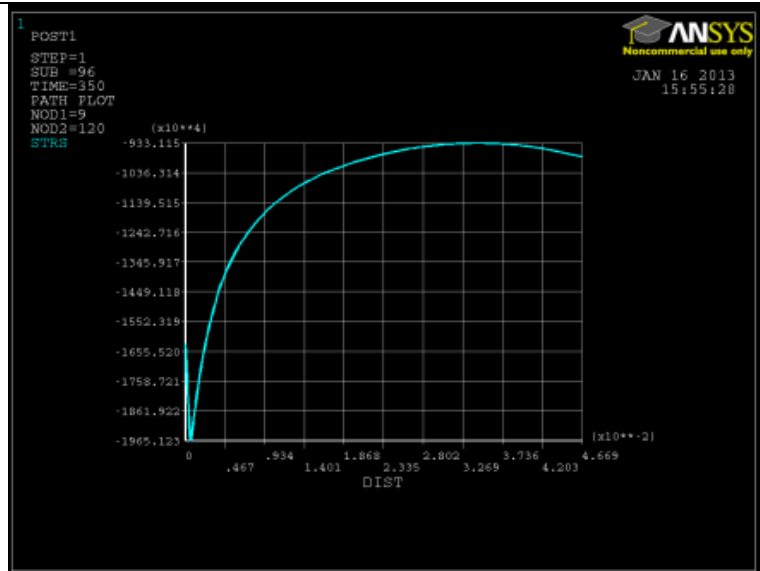
Maximum residual stress- -48.78MPa

9.2 tool $\mu=0.75$ $\delta=0$



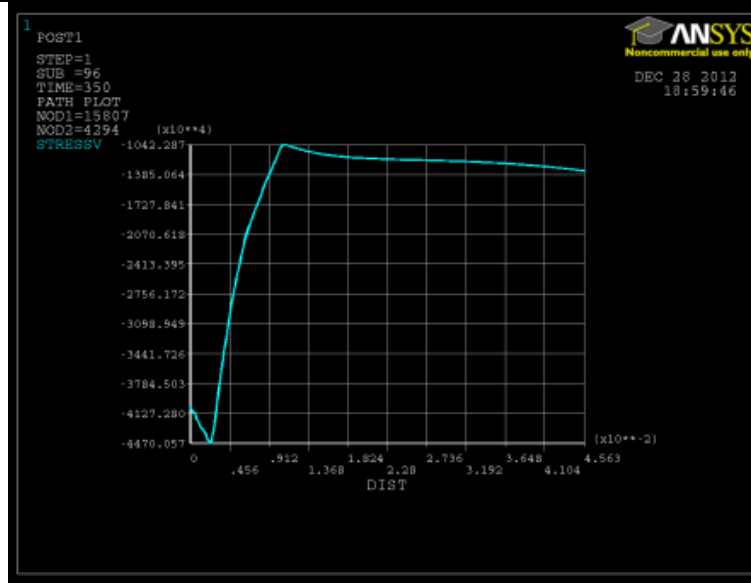
Maximum residual stress- -42.4

9.2 tool $\mu=0.75$ $\delta=0.25$



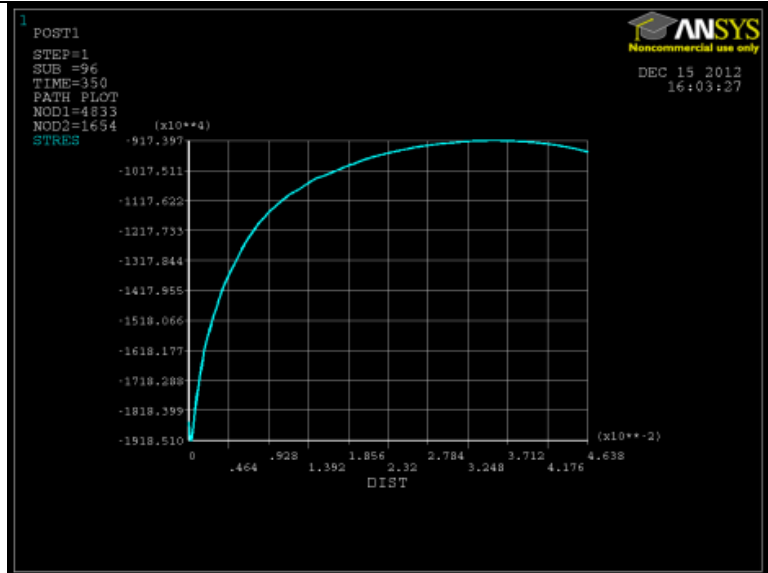
Maximum residual stress- -19.6

9.2 tool $\mu=0.75$ $\delta=0.5$



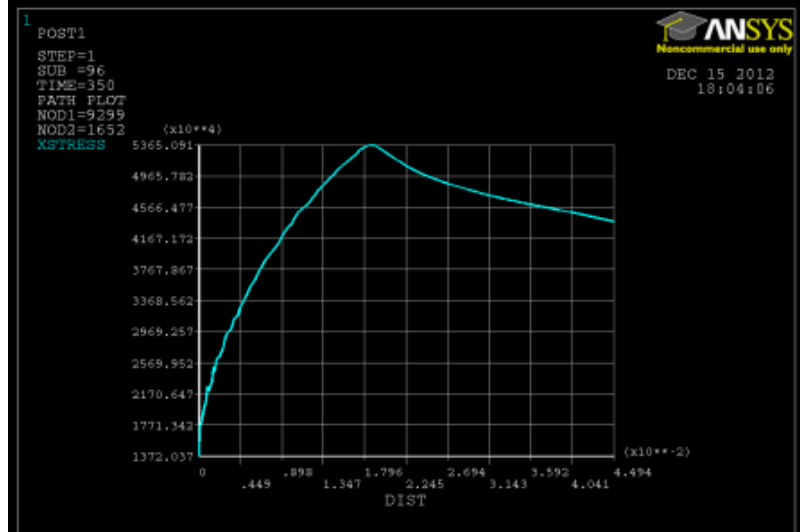
Maximum residual stress- -44.7

9.2 tool $\mu=1$ $\delta=0$



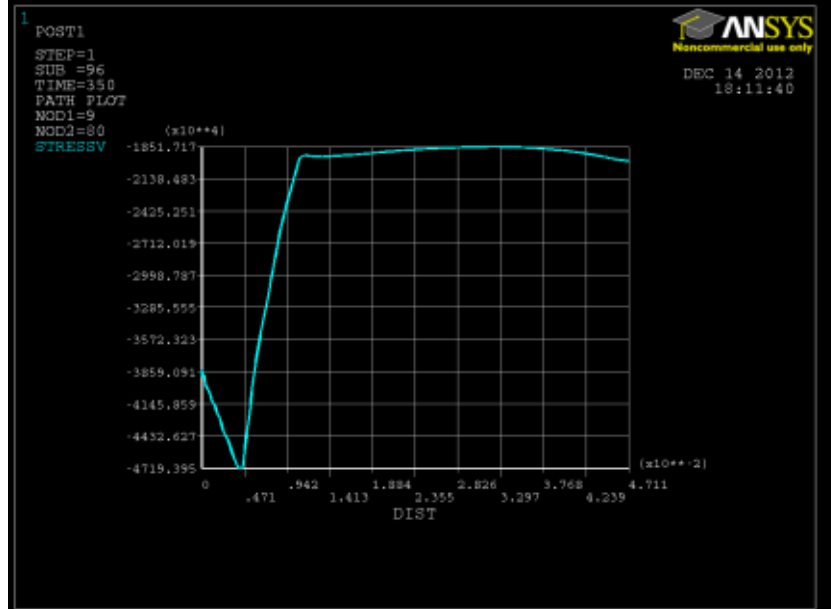
Maximum residual stress- -19.18

9.2 $\mu=1$ $\delta=0.5$



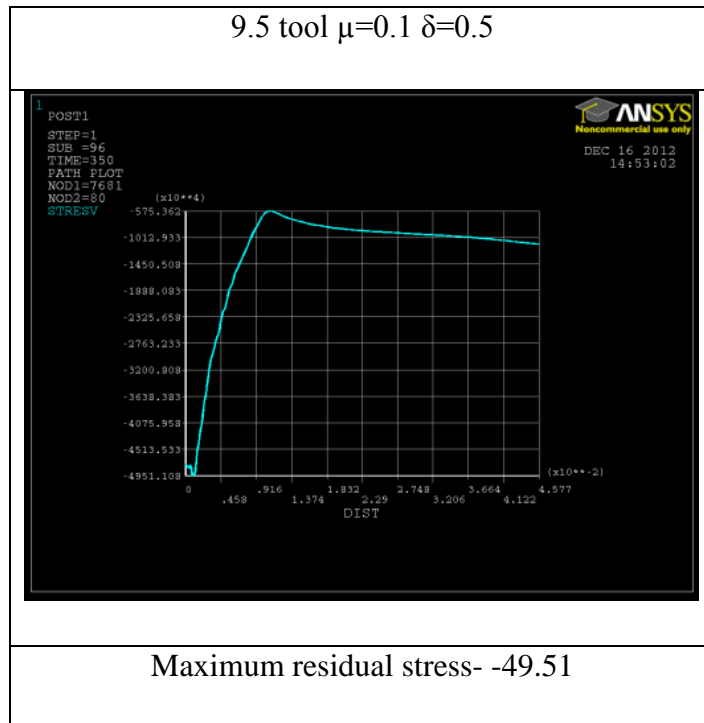
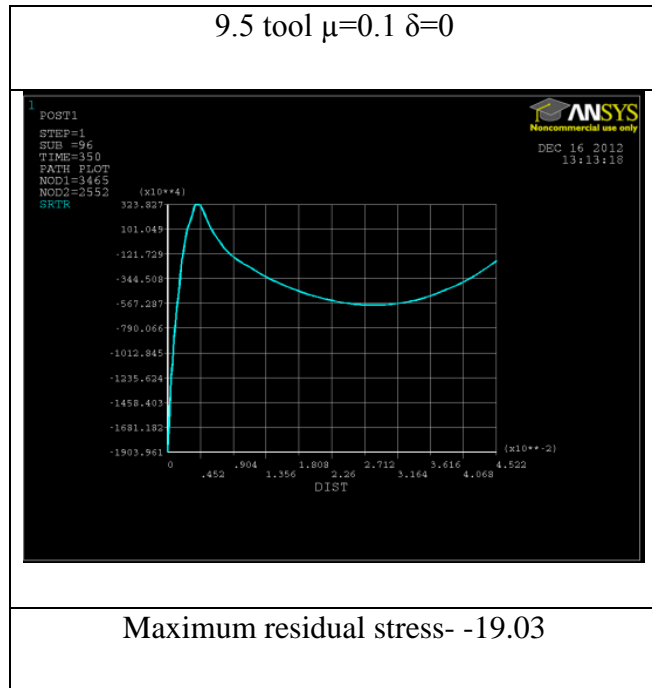
Maximum residual stress- -8.79MPa

9.2 $\delta=1$

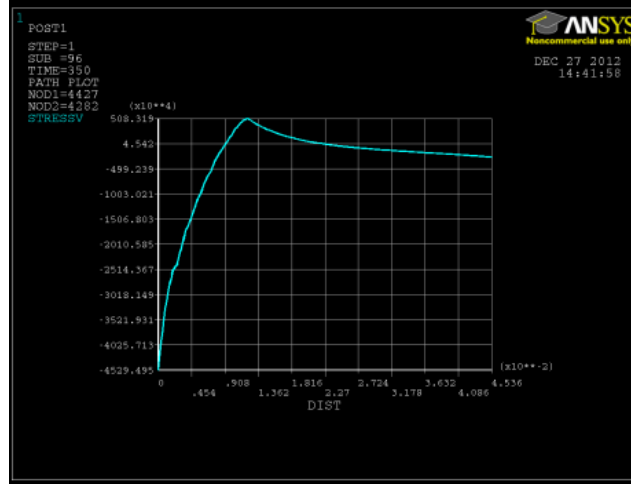


Maximum residual stress- -47.92

Results for 9.5 Tool:

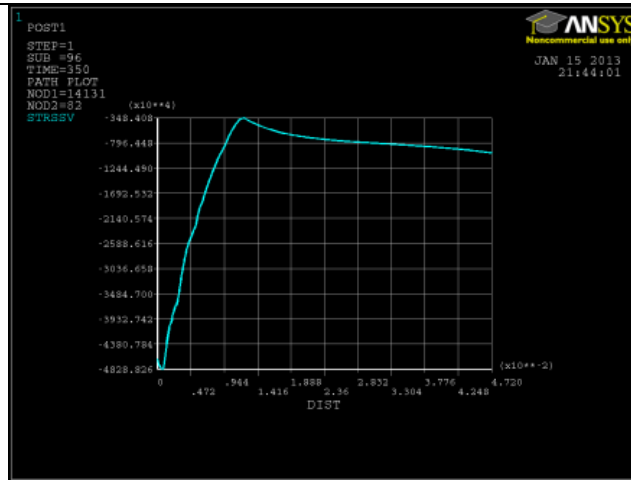


9.5 tool $\mu=0.25$ $\delta=0$



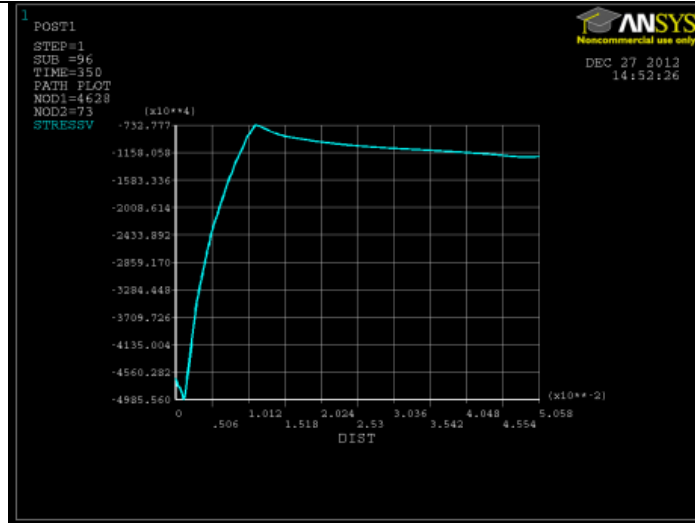
Maximum residual stress- -45.3

9.5 tool $\mu=0.25$ $\delta=0.25$



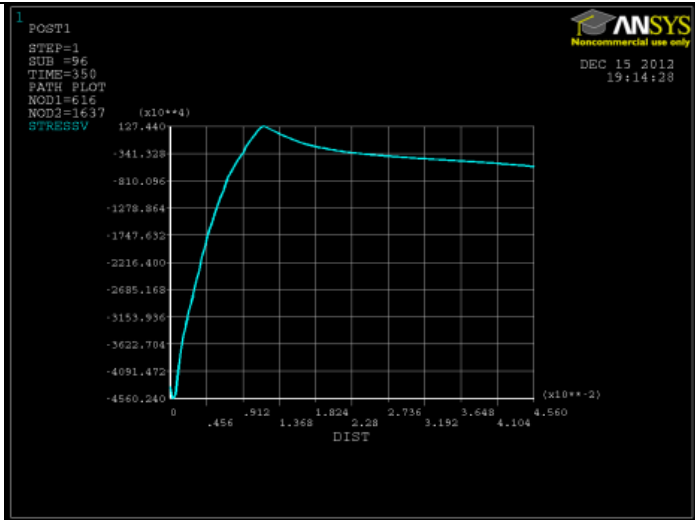
Maximum residual stress- -48.55

9.5 tool $\mu=0.25$ $\delta=0.5$



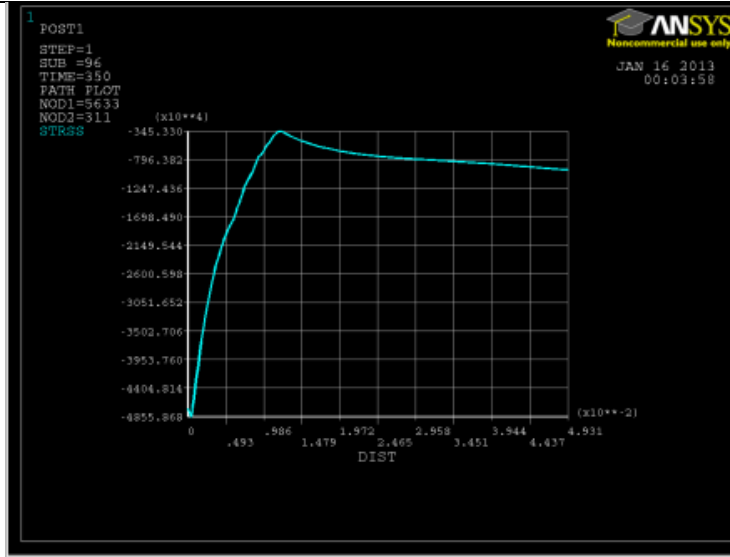
Residual stress -49.8 MPa

9.5 $\mu=0.5$ $\delta=0$



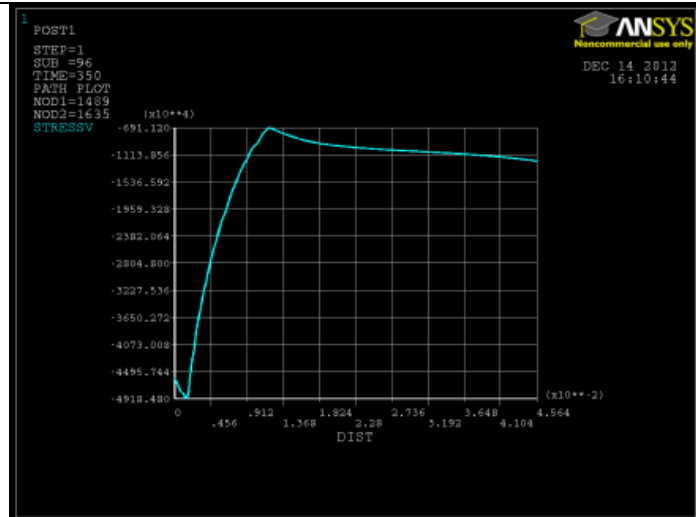
Maximum residual stress -49MPa

9.5 $\mu=0.5$ $\delta=0.25$



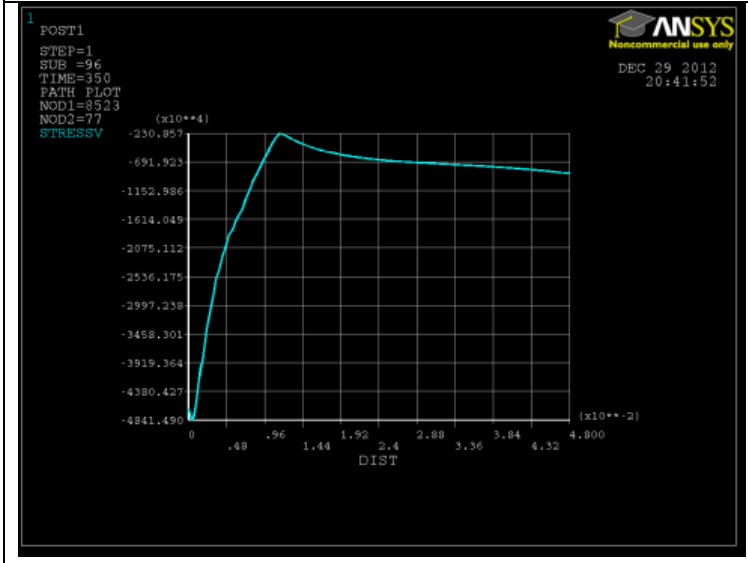
Maximum Residual stress -48.3 MPa

9.5 $\mu=0.5$ $\delta=0.5$



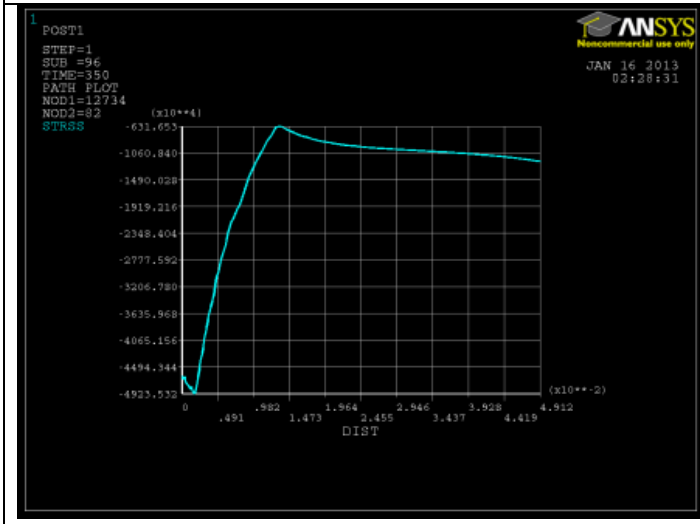
Maximum Residual stress -49.18 MPa

9.5 $\mu=0.75$ $\delta=0$



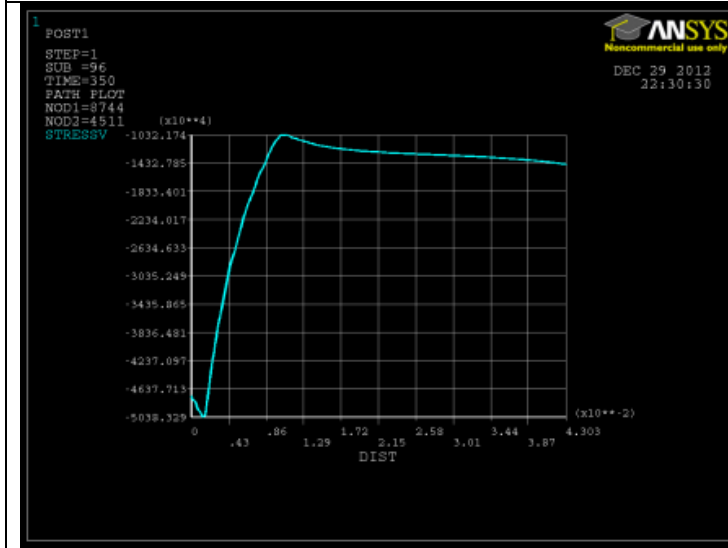
Maximum Residual stress -48.14 MPa

9.5 $\mu=0.75$ $\delta=0.25$



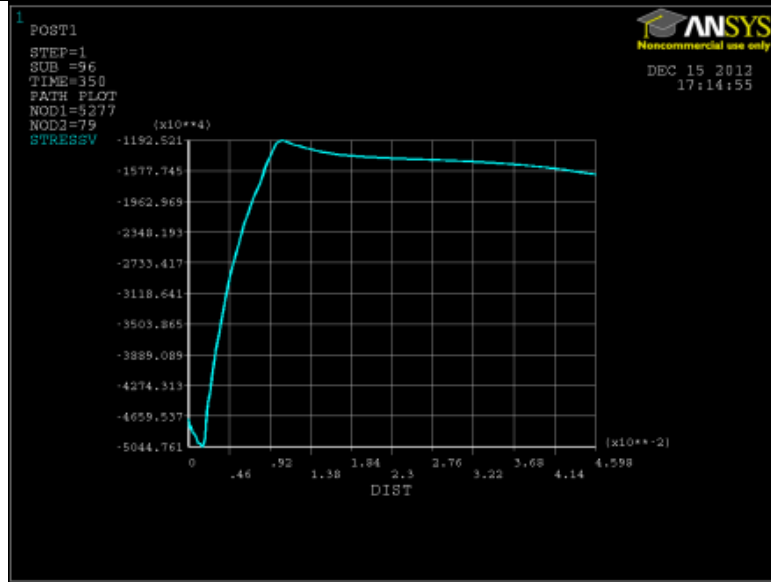
Maximum Residual stress -49.3

9.5 $\mu=0.75$ $\delta=0.5$



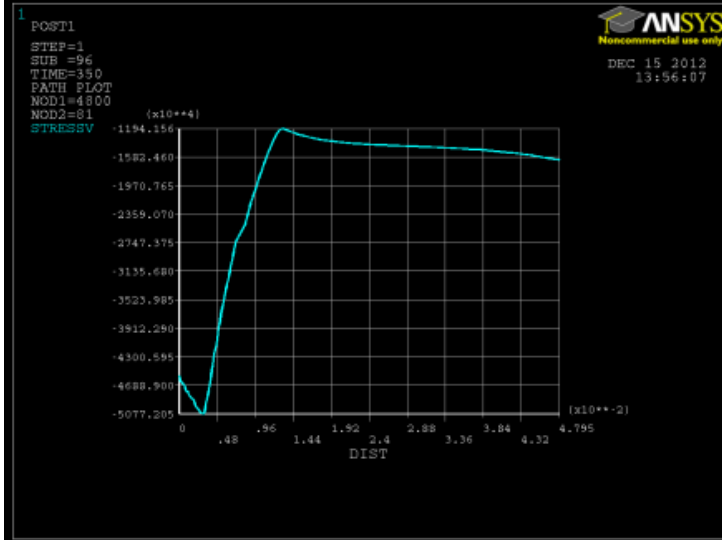
Maximum Residual stress -48.41

9.5 $\mu=1$ $\delta=0$



Maximum Residual stress -50.44

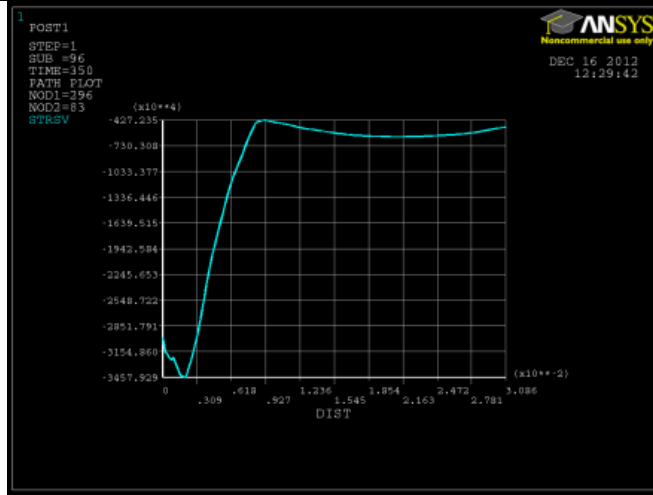
9.5 $\mu=1$ $\delta=0.5$



Maximum Residual stress -50.77

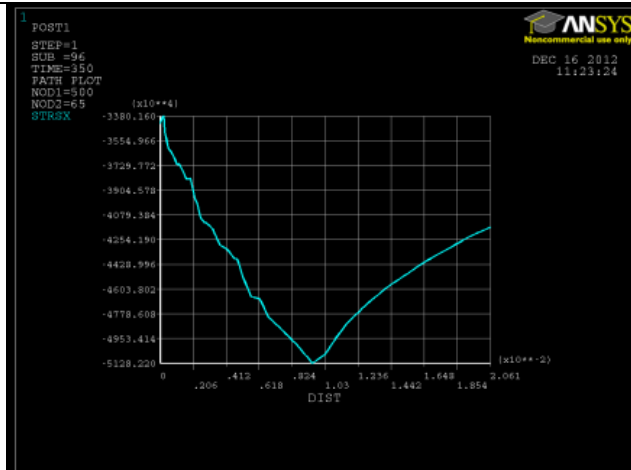
Results for 9.9 tool:

9.9 $\mu=0.1$ $\delta=0$



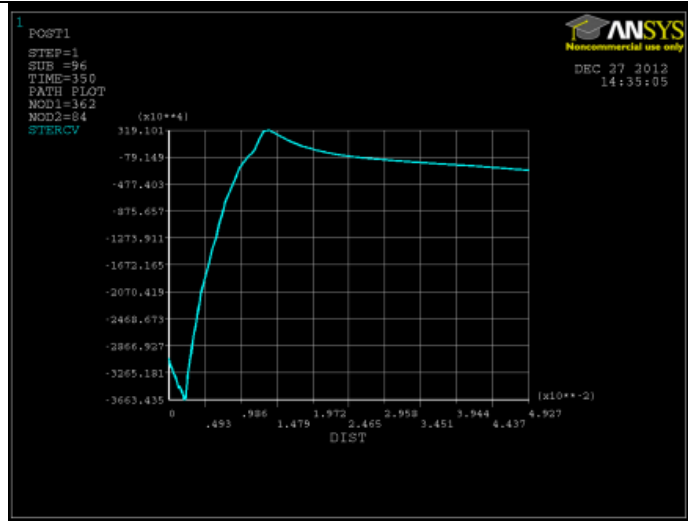
Maximum Residual stress -34.6 MPa

9.9 $\mu=0.1$ $\delta=0.5$



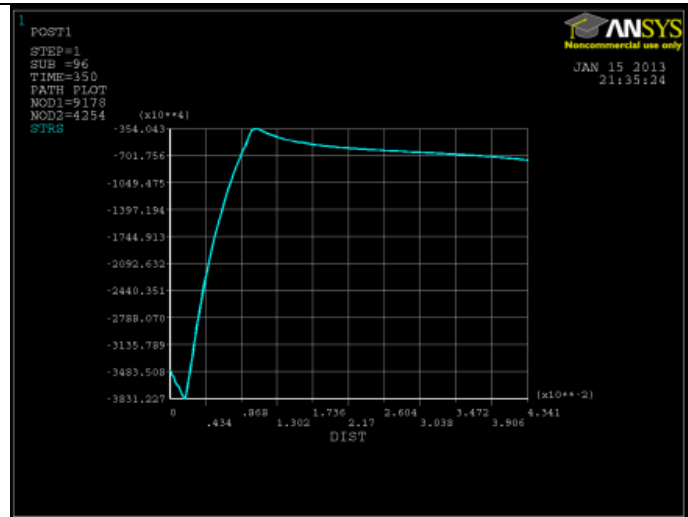
Maximum Residual stress -51.28

9.9 $\mu=0.25$ $\delta=0$



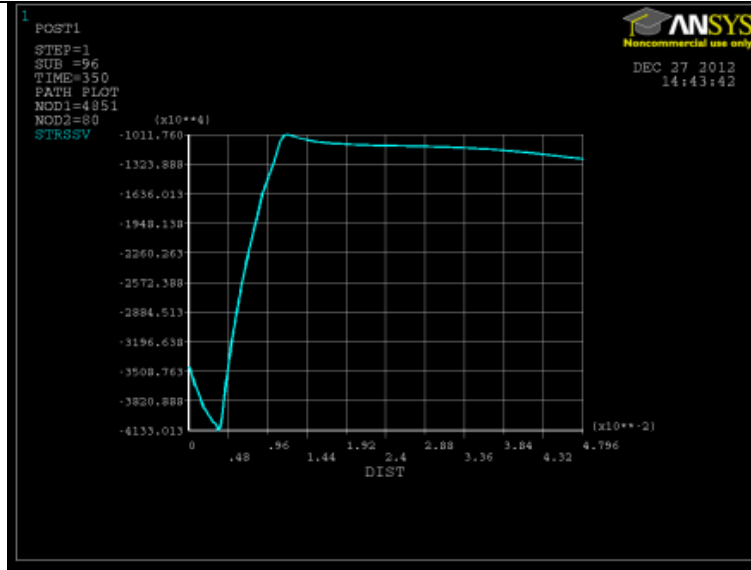
Maximum Residual stress -36.63 MPa

9.9 $\mu=0.25$ $\delta=0.25$



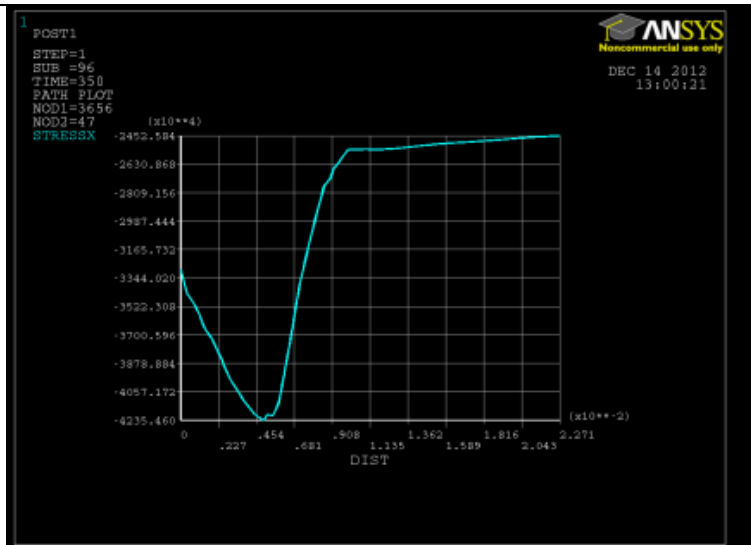
Maximum Residual stress -38.31 MPa

9.9 $\mu=0.25$ $\delta=0.5$



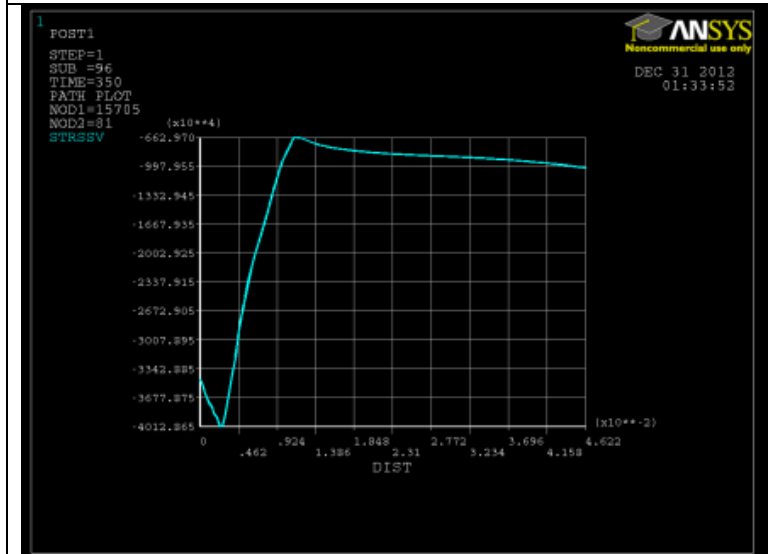
Maximum Residual stress -41.33MPa

9.9 tool $\mu=0.5$ $\delta=0$



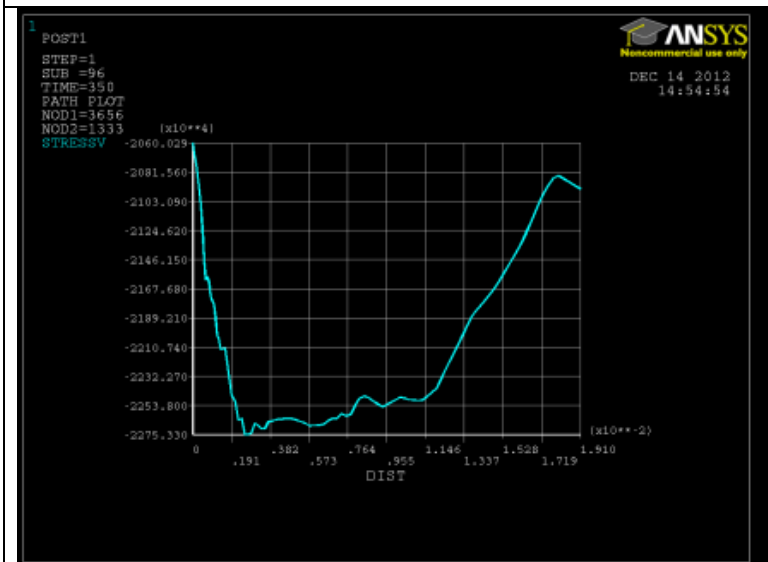
Maximum Residual stress -42.35MPa

9.9 tool $\mu=0.5$ $\delta=0.25$



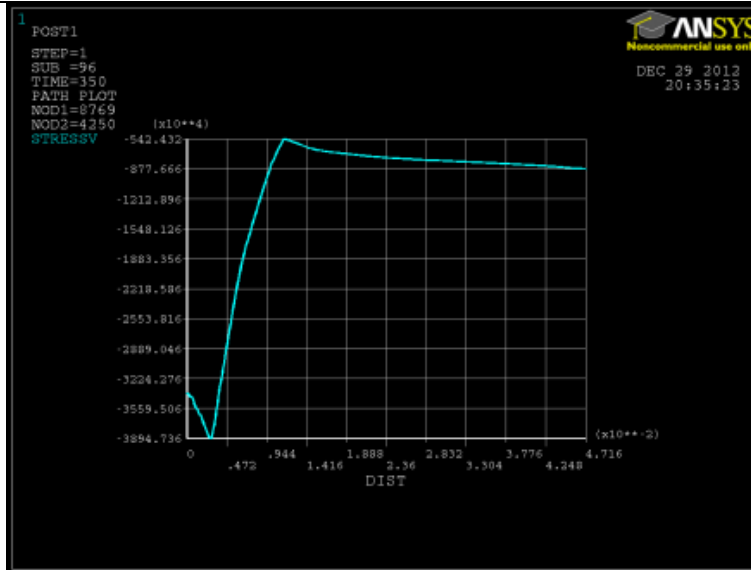
Maximum Residual stress -40.12MPa

9.9 tool $\mu=0.5$ $\delta=0.5$



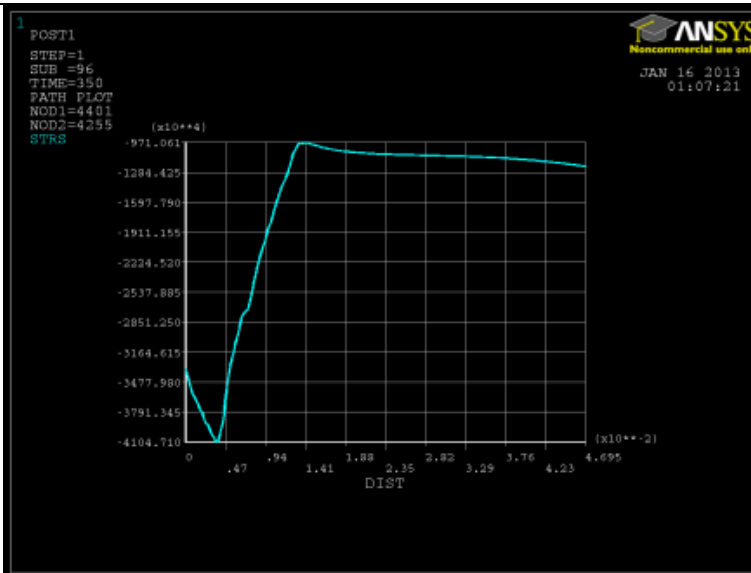
Maximum Residual stress -22.75MPa

9.9 tool $\mu=0.75$ $\delta=0$



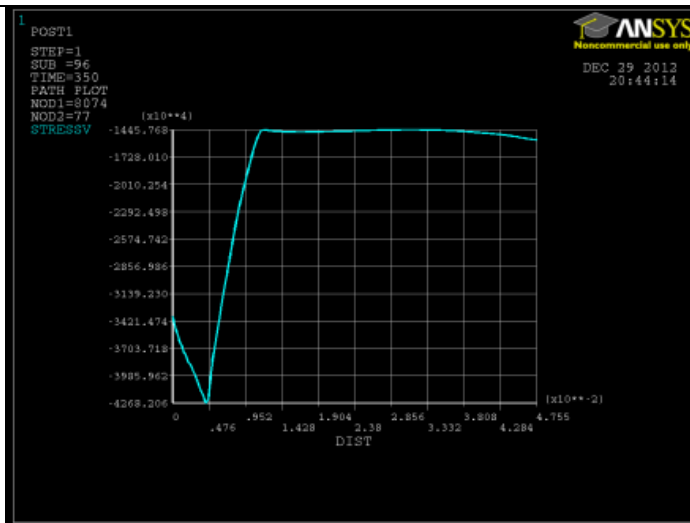
Maximum Residual stress -38.94 MPa

9.9 tool $\mu=0.75$ $\delta=0.25$



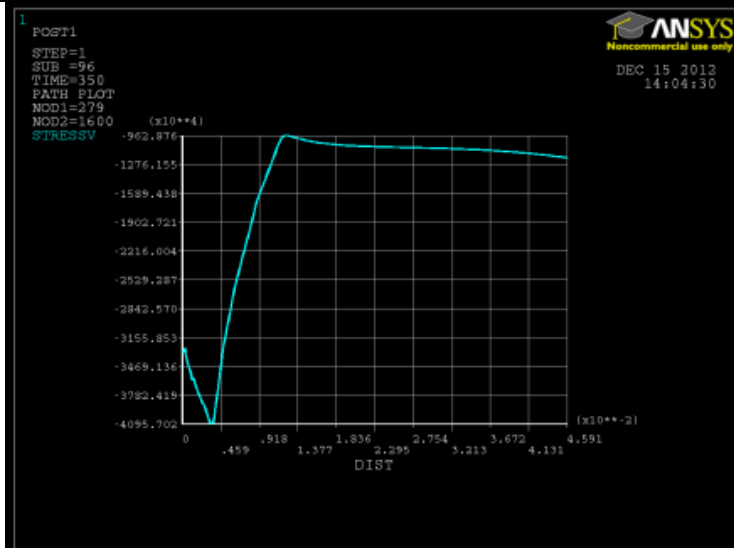
Maximum Residual stress -41.04 MPa

$9.9 \mu = 0.75 \quad \delta = 0.5$



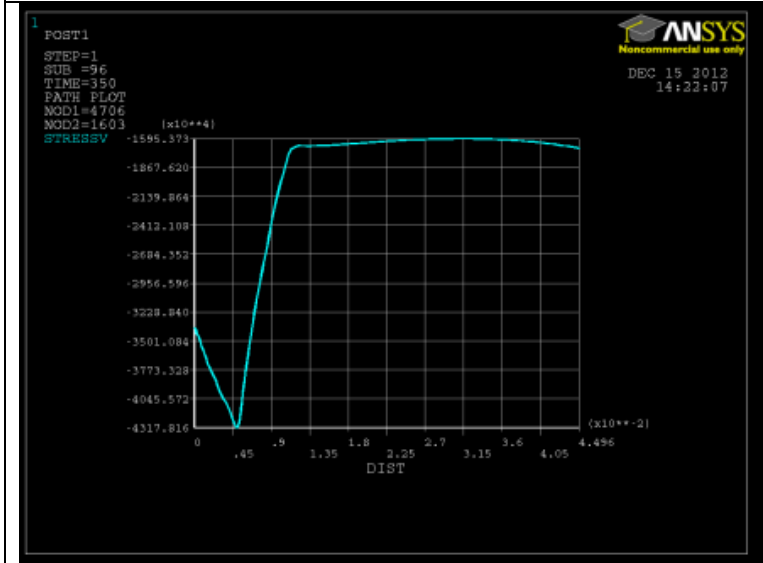
Maximum Residual stress -42.68 MPa

$9.9 \mu = 1 \quad \delta = 0$



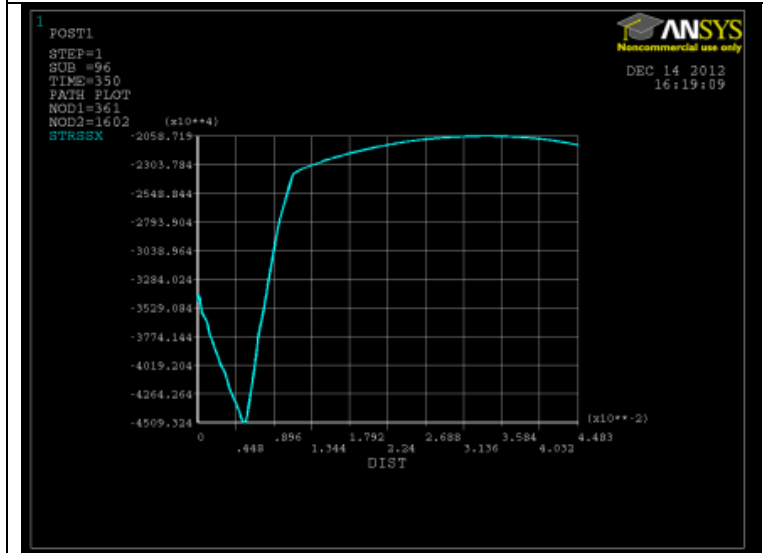
Maximum Residual stress -40.95 MPa

$$9.9 \mu = 1 \delta = 0.5$$



Maximum Residual stress -43.17MPa

$$9.9 \delta = 1$$



Maximum Residual stress -45MPa